Does limestone show useful optically stimulated luminescence?

R. B. Galloway
Department of Physics and Astronomy, The University of Edinburgh, Mayfield Road, Edinburgh EH9 3JZ, Scotland, U.K.

(Received 6 March 2002; in final form 6 May 2002)

Abstract: *Luminescence around 515 nm wavelength (2.41 eV) from limestone stimulated by pulsed light of 370 nm wavelength (3.36 eV) is found to decrease with increasing radiation dose.*

Introduction

Liritzis (1994) proposed a method for dating the construction of megalithic limestone buildings, based on the latent thermoluminescence of the surface of a limestone building block being bleached by exposure to light prior to incorporation in the building and then, in the inter-block surfaces from which light is excluded, growing again with the passage of time in a manner akin to the well known methods of dating sediment deposition using quartz or feldspar extracts, for example Wintle and Huntley (1980). The method has since given an age for the Temple of Apollo in Delphi consistent with the historical age (Liritzis *et al.*, 1997), and has been applied to determine the age of two Greek pyramids (Theocaris *et al.*, 1997). Liritzis and Bakopoulos (1997) observed the decrease in the thermoluminescence peak at 280ºC with exposure to sunlight for several samples of Greek limestone. However, a substantial residual signal was found after 100 hours of exposure. Just as the use of optically stimulated luminescence rather than thermoluminescence is advantageous with quartz or feldspar when dating sediments (e.g. Huntley *et al.*, 1985), the same advantage, namely the absence of residual signal from bleached material, could be hoped for if optically stimulated luminescence could be used with limestone. Wintle (1997), in a review of luminescence dating procedures, drew attention to the report by Ugumori and Ikeya (1980) of the optical stimulation of luminescence from $CaCO_3$ and noted that no further work on the topic had been reported. Ugumori and Ikeya (1980) observed luminescence (a broad band around 430 nm, 2.9 eV) stimulated by light from a N_2 laser (337 nm, 3.68 eV) from natural calcite, both crystalline and a piece of stalactite. The potential for archaeological dating was illustrated by an increase in luminescence intensity with increasing distance from the surface into the stalactite. Exposure to the laser light altered the thermoluminescence glow curve, reducing the peak at 347˚C, increasing the peaks at 287˚C and 237˚C, and creating a peak at 57˚C.

The work reported here was developed independently from the study of the bleaching and phototransfer properties of the 286˚C peak in the thermoluminescence glow curve from limestone (Bruce *et al.*, 1999). This is the dominant peak in the thermoluminescence glow curve from limestone and the peak used for dating megalithic buildings (Liritzis, 1994; Theocaris *et al.*, 1997). Bruce *et al.* (1999) found that the bleaching of the 286˚C peak by light in the wavelength range 350 – 600 nm was more rapid for shorter wavelengths of light, 350 – 400 nm being most effective and wavelengths longer than 500 nm having little effect. Accordingly for the present measurements, a Nichia light emitting diode (LED) with peak emission at 370 nm (3.36 eV) was used as stimulating light source.

Experimental details

The source of stimulating ultraviolet light was a Nichia LED type NSHU590E, which according to the manufacturer's data has a peak emission at 370 nm, a half-width of 12 nm, with the output intensity falling to about 1% at 360 and 410 nm, a power output of 750 μW, and an emission angle of 10º. Measurements with a spectrophotometer over the wavelength range 400-800 nm show a tiny emission relative to the ultraviolet output, which would however be quite significant at the level of photon counting, with a wide peak around 550 nm and a narrower peak around 750 nm. This unwanted emission in the visible region is greatly reduced by a Schott 7-60 optical filter (peak transmission at 370 nm, falling to 0.01% at 405 nm), which was mounted in front of the LED for all the measurements reported below, fig.1.

Green light emitted from the sample was selected by a combination of HA3, BG39 and GG495 optical filters (peak transmission 515 nm, half maximum at

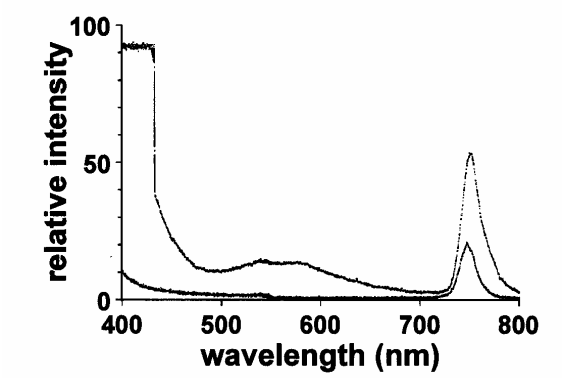

Figure 1.
The visible spectrum from a Nichia type NSHU590E LED compared with a spectrum of the light which has passed through a Schott 7-60 filter. The constant relative intensity of 93 from 400 to 430 nm in the unfiltered spectrum is due to high light intensity causing saturation of the detector.

495 and 600 nm, 0.01% at 480 and 780 nm) and detected by a 9635QA photomultiplier, the same arrangement as in the dating work by Liritzis (1994), Theocaris *et al.* (1997) and the bleaching study by Bruce *et al.* (1999).

The same French limestone, treated with dilute acetic acid to avoid spurious luminescence following Wintle (1975), as used by Bruce *et al.* (1999) was used for the present measurements. The grain size was ~ 100 μm.

The background counting rate with the LED on and a clean stainless steel disc in the sample position was ~2.6×10^5 s^{-1} which fell to less than half within 50 ms of the LED being switched off. This high background counting rate is attributed to fluorescence from the optical filters. No significantly higher counting rate was observed with natural limestone on the stainless steel disc, but on switching off the LED, it took about 250 ms for the light to fall to half of the maximum intensity. It was decided therefore to avoid the high background counting rate while the LED was on by using pulsed stimulation and to look for decaying luminescence after the end of the stimulating pulse, in the manner of the measurements on α-Al_2O_3:C by Bulur and Göksu (1997). The LED was pulsed on once for 1 s and photon counting for luminescence detection started at the end of the pulse for 250 successive intervals of 50 ms. Successive measurements were essentially identical, as shown below. The equipment was that used in this laboratory for thermoluminescence measurement (Galloway, 1990), with minor modification to the connections and controlling programme to pulse the LED rather than operate the heater.

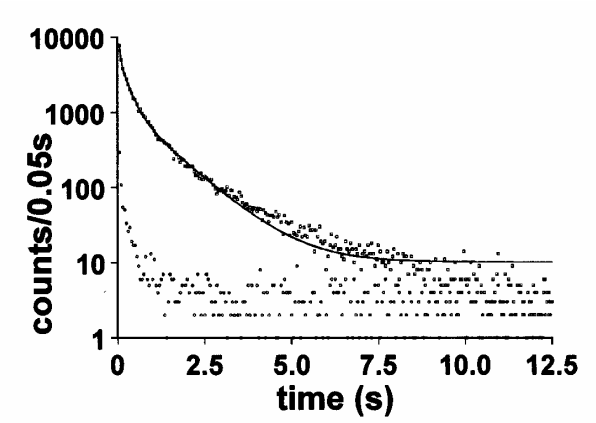

Figure 2.
Comparison of the time dependence of the light from a natural limestone sample with that from a stainless steel disc, following a pulse of ultraviolet from the LED of 1 s duration. The curve is a least squares fit to the data of a sum of three exponentials plus a constant with the parameters in table 1.

The measurements

With the pulsed system the signal from natural limestone stands out clearly from the measurement made with an empty disc, fig.2. The decay of luminescence after the end of the stimulating pulse follows Σ_i $A_i \exp(-t/\tau_i)$ (plus a small constant background) where τ_i are the lifetimes associated with the luminescence processes in the crystal and A_i are the amplitudes of the components, and the curve in fig. 2 shows a least squares fit of this expression to the data with lifetimes of 0.04, 0.25 and 1.06 s. Each component will increase exponentially during the stimulating pulse, reaching 95% of the maximum possible amplitude in 3 lifetimes of stimulation. Thus, shortening the stimulating pulse should emphasise the shorter lifetime components and lengthening the stimulating pulse should emphasise the longer lifetime components. This is found to be so, comparing stimulation by pulses of duration 0.1, 1.0 and 10 s in fig. 3, with the luminescence decaying more rapidly the shorter the pulse and the data being fitted by the parameters in table 1.

Stimulating pulse duration (s)	0.1	1.0	10
τ_1 (s) [relative amplitude]	0.04 [0.76]	0.04 [0.62]	0.05 [0.55]
τ_2 (s) [relative amplitude]	0.21 [0.21]	0.25 [0.29]	0.29 [0.33]
τ_3 (s) [relative amplitude]	0.93 [0.03]	1.06 [0.08]	1.36 [0.12]

Table 1.

Parameters resulting from least squares fitting of the data in fig. 3 for the decay of luminescence after the end of the stimulating pulse by $\Sigma_i A_i \exp(-t/\tau_i)$ (plus a small constant background), where τ_i are the lifetimes associated with the luminescence processes in the crystal and A_i are the amplitudes of the components. The relative amplitude is quoted below, $A_i/\Sigma_i A_i$. In each case there were only 3 statistically significant components.

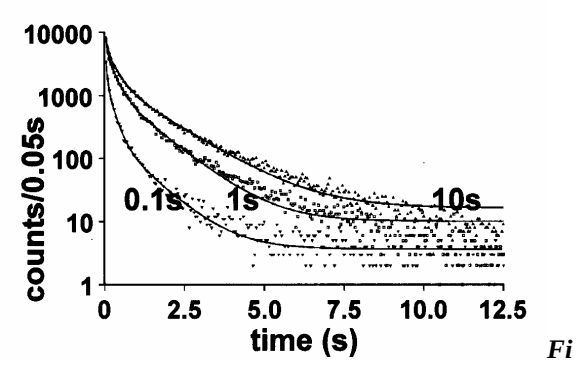

Fi

Figure 3.

Comparison of the time dependence of the light from a natural limestone sample following pulses of ultraviolet from the LED of 0.1, 1.0 and 10 s duration. The curves are least squares fits to each data set of a sum of three exponentials plus a constant, with the parameters in table 1.

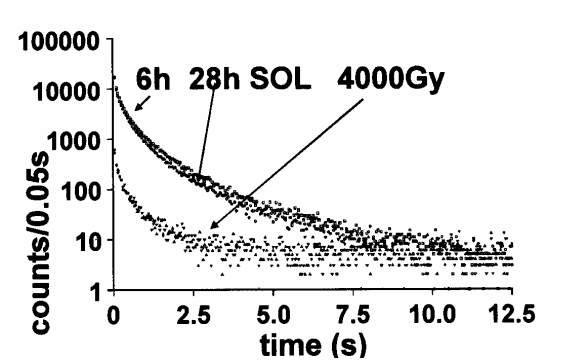

Figure 4.

Comparison of the time dependence of the light, following a 1 s duration ultraviolet pulse, from the limestone sample after 6 hours and 28 hours in a SOL-2 solar simulator and after a subsequent beta exposure of 4000Gy (for which the indistinguishable data from two successive measurements are shown).

The natural limestone sample used to produce fig. 2 was subsequently "bleached" in a SOL-2 solar simulator for 6 hours, the pulsed OSL measured, then bleached for a further 22 hours and the pulsed OSL measured, fig. 4. There is only a little difference between the results from 6 hours and 28 hours total bleaching, but the signal is increased compared with the signal from the natural limestone, fig. 2. The sample was then irradiated by beta particles to a dose of 4000 Gy and the pulsed OSL measured, giving a substantially smaller signal than after bleaching, fig. 4. Comparing the pulsed OSL signal from a limestone sample immediately it was removed from the SOL-2 after several months of exposure with the signal from the same sample after beta irradiation to a dose of 40 Gy, shows little change in signal immediately after the stimulating pulse, while beta irradiation to 800 Gy shows a clear reduction in signal, fig. 5.

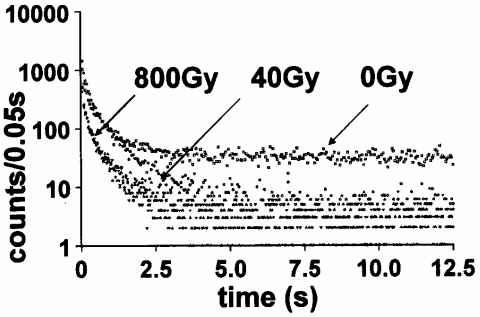

Figure 5.

The time dependence of light, following a 1 s duration ultraviolet pulse, from a limestone sample immediately after several months in the SOL-2 solar simulator, along with data for the same sample after receiving a beta dose of 40 Gy and 800 Gy (for which the indistinguishable data from 3 successive measurements are shown).

The data from the sample taken immediately from the SOL-2, fig. 5, have a higher constant background level than the other data, possibly due to phosphorescence induced by the light exposure in the SOL-2.

In general, measurements can be repeated without detectable loss of signal, as illustrated for the 4000Gy added dose data in fig. 4 and for the 800 Gy data in fig. 5.

Limestone which has been heated to 500˚C before investigation behaves similarly, (maximum counting rate 4.8×10^5 s^{-1}, after 60 Gy beta dose 4×10^5 s^{-1} maximum, both with a similar decay to the bleached material).

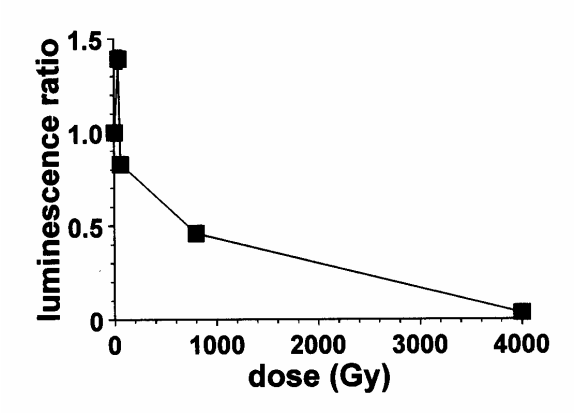

Figure 6.
The dependence on radiation dose of the luminescence detected during the 50 ms immediately following switch off of the stimulating light. The luminescence ratio plotted is the number of luminescence counts from a sample which has received a radiation dose to the number of luminescence counts from the same sample after bleaching for at least 24 hours in the SOL-2.

Discussion

Figs. 2, 4 and 5 show that limestone does not provide optically stimulated luminescence which increases with radiation dose, to permit dating in a manner similar to that employed with quartz or feldspar, at any rate not with the wavelength of stimulating light and the wavelength of detected luminescence used in this work. In contrast, the work by Ugumori and Ikeya (1980) indicated an increase in optically stimulated luminescence with radiation dose, but used a different stimulating wavelength (337 nm compared with 370 nm in the present work) and a different wavelength of luminescence (430 nm compared with 515 nm in the present work). Further, the Ugumori and Ikeya (1980) study related to the 347˚C peak in the thermoluminescence glow curve, whereas the present study related to the 286˚C peak.

The general trend in the measurements reported here is for the intensity of optically stimulated luminescence to fall with increasing radiation dose, shown quantitatively in fig. 6 for the luminescence detected in the 50 ms immediately following the switch off of the stimulating light, although there may be a small increase in luminescence up to about 50 Gy dose. This behaviour is reminiscent of the infrared radioluminescence of feldspar (Krbetschek *et al.*, 2000), which has been exploited for sediment dating. Whether the phenomenon shown by limestone in fig. 6 could be used for equivalent dose determination for the purpose of dating would require further investigation of the reproducibility of the data, the dependence of the luminescence signal on bleaching time and confirmation that the signal does relate to electrons trapped with long term stability appropriate to dating. A hint that the latter may be true is given by the luminescence from the natural limestone which, measured in the same way as the points in fig. 6, gives a luminescence ratio of 0.45 which would correspond to an equivalent dose of 800 Gy. However with regard to the problem which initiated this investigation, the dating of limestone buildings, the equivalent dose to be determined is typically less than 20 Gy (Theocaris *et al.*, 1997), which would require a much more detailed study of the phenomenon in fig. 6 for small radiation dose values.

Conclusion

Does limestone show useful optically stimulated luminescence? For the wavelengths of stimulation and detection studied, not immediately, but there is an indication of a way forward.

References

Bruce, J., Galloway, R.B., Harper, K. and Spink, E. (1999). Bleaching and phototransfer of thermo-luminescence in limestone. *Radiat. Meas*. **30**, 497-504.

Bulur, E. and Göksu, H.Y. (1997). Pulsed optically stimulated luminescence from α-Al_2O_3:C using green light emitting diodes. *Radiat. Meas.* **27**, 479-488.

Galloway, R.B. (1990). Notes on a recently constructed TL system. *Ancient TL* **8**(2), 10-11.

Huntley, D.J., Godfrey-Smith, D.I. and Thewalt, M.L.W. (1985). Optical dating of sediments. *Nature,* **313**, 105-107.

Krbetschek, M.R., Trautmann, T., Dietrich, A. and Stolz, W. (2000).Radioluminescence dating of sediments: methodological aspects. *Radiat. Meas* **32**, 493-498.

Liritzis, I. (1994). A new dating method by thermoluminescence of carved megalithic stone building. *Comptes Rendus de l'Académie des Sciences Paris*, serie II **319**, 603-610.

Liritzis, I. and Bakopoulos, Y. (1997). Functional behaviour of solar bleached thermoluminescence in calcites. *Nucl. Instrum. and Meth.*, **B132**, 87-92.

Liritzis, I., Guibert, P., Foti, F. and Schvoerer, M. (1997). The Temple of Apollo (Delphi) strengthens novel thermoluminescence method. *Geoarchaeology*, **12**, 479-496.

Theocaris, P.S., Liritzis, I. and Galloway, R.B. (1997). Dating of two Hellenic pyramids by a novel application of thermoluminescence. *J. Archaeol. Sci*. **24**, 399-405.

Ugumori, T. and Ikeya, M. (1980). Luminescence of $CaCO_3$ under N_2 laser excitation and application to archaeological dating. *Japanese Journal of Applied Physics* **19**, 459-465.

Wintle, A.G. (1975). Effects of sample preparation on the thermoluminescence characteristics of calcite. *Modern Geology* **5**, 165-167.

Wintle, A.G. (1997). Luminescence dating: Laboratory procedures and protocols. *Radiat. Meas.* **27**, 769-817.

Wintle, A.G. and Huntley, D.J. (1980). Thermoluminescence dating of ocean sediments. *Can. J. Earth Sci.* **17**, 348-360.

Reviewer
Ann Wintle

Thick source alpha counting: the measurement of thorium

H. Sjostrand[1] and J.R. Prescott[2]
Physics and Mathematical Physics, University of Adelaide, Australia 5005
[1]present address: Department of Neutron Research, Uppsala University, 75120 Uppsala, Sweden
[2]corresponding author, email: john.prescott@adelaide.edu.au

(Received in final form 20 June 2002)

Introduction

From time to time, in papers from our laboratory, we have discussed the technique of thick source alpha particle counting (TSAC) for determining uranium and thorium concentrations and hence dose rates, more particularly as it relates to its use in luminescence and ESR dating (e.g. Jensen and Prescott 1983, Akber et al 1983, Woithe and Prescott 1995 (hereinafter, Woithe and Prescott without the date).

In the last-mentioned of these references we discussed the question of the efficiency of the zinc sulphide screens used in the method. In summary, we presented evidence that the effective efficiency is not only less than 100% but varies a percent or two from batch to batch of screens. A typical efficiency was shown to be between 85% and 90% for the screens supplied commercially by W.B. Johnson. This work was undertaken because of a widely expressed belief that the efficiency is 100%.

At the time of publication of Woithe and Prescott, the reviewer, Huntley, commented that the paper made a case that, "all is not well" and made a number of suggestions about methodology, all of which had already been incorporated into the project. Huntley also remarked that, in his own use of TSAC (Huntley et al, 1986) he finds efficiencies of close to 100% for standards, although thorium seems to be underestimated, and he applies a correction for this. As mentioned in Woithe and Prescott, the late John Hutton had also derived an empirical correction for underestimation of thorium.

TSAC : the method

It will be useful briefly to recall the process of calibrating TSAC with a zinc sulphide screen and photomultiplier, as originally set out by Aitken (1985 Appendix J). Using a certified U or Th standard in known geometry, the count rate is measured as a function of discriminator setting. The discriminator setting for subsequent practical use is set at 85% of the extrapolated counting rate for Th and 82% for U. With this setting, the count rate for the standard should correspond to that predicted by Aitken's calculations or corresponding calculations by others. If the observed count rate is less than that predicted, it is concluded that the efficiency of the zinc sulphide screen is less than 100% and its value is determined. This was the procedure in Woithe and Prescott.

Our contention remains that, when calibration is carried out with standard sources according to the original prescription of Aitken (1985) but using updated conversion factors, with finely ground samples (Jensen and Prescott, 1983) an efficiency of less than 100% is found. Woithe and Prescott used the conversion factors of Huntley et al (1986) and found efficiencies between 85% and 90%.

The most recent calculation relating concentrations of U and Th with count rates for a particular geometry is that of Adamiec and Aitken (1998). Their factors are smaller than those of Huntley et al (1986) by about 6%. Since these conversion factors are used in calibrating the counting system and finding the efficiency of the screens, the effect of applying the Adamiec and Aitken conversion factors would be to increase the measured efficiency of the screens by 6%. In our case, all would now be now better than 90%.

In fact, from the point of view of calculating dose-rates for luminescence dating, the conversion factors are not critical since they are used in both the calibration and the subsequent alpha counting of samples. Provided that a corresponding screen efficiency is used, the measurement is essentially a comparison with the standard. This is not true, of course, if the efficiency is wrongly assumed to be 100%. There is a further caveat for efficiencies less than 100%: The pairs counting technique requires the detection of two alpha particles, which follow each other in the thorium decay chain. Consequently a

correction for both requires the efficiency correction factor to be squared.

Methodology of the measurement of thorium

We have now returned to the problem from a different angle, concentrating on a comparison of two independent measurements of thorium concentration viz, TSAC and neutron activation analysis (NAA). We show that our deduction of an efficiency of less than 100% is sustained. Further, incorporation of delayed neutron activation (DNA) measurements of uranium improves the TSAC estimate of thorium.

In the standard usage of TSAC, the total combined count rate, for thorium with its daughters and uranium with it daughters, is recorded. In addition "slow pairs" record successive alpha decays of ^{220}Rn and its daughter ^{216}Po in the thorium decay chain and hence give a measure of the concentration of thorium. Since the rate of slow pairs is commonly about 3% of the total alpha count rate, the statistical accuracy is necessarily low for counting times of a day or two. Nevertheless, in calculating dose-rates from alpha-counting data, some measure of the ratio of uranium to thorium is better than no estimate at all, or a guess.

Of course, for luminescence and ESR dating, the important quantity is the dose-rate, which is derived from the U, Th and K concentrations together with cosmic ray intensity. For a given total alpha particle count, the dose-rate is very insensitive to the relative amounts of Th and U (Sasidharan et al 1978; Aitken 1990).

In the present paper, we compare the thorium concentrations obtained by TSAC with those obtained by NAA. In the first instance we have chosen to stay with our original (Huntley et al 1986) conversion factors.

Results

"Raw" Pairs Counting

Samples were selected, more or less at random, from our data set to cover the range of thorium concentrations from less than 1 $\mu g.g^{-1}$ to about 30 $\mu g.g^{-1}$. Initially, all samples were field samples, collected in the course of dating assignments from a variety of sites in Australia, Europe, Thailand and China. All samples had been analysed by TSAC, DNA and NAA. A few analyses were repeated. With exceptions noted below, samples known or suspected to be in radioactive disequilibrium were excluded. Such samples have been thought to be rare in our experience. However, interestingly, when all the data were assembled, five samples were found to give inconsistent uranium analyses. Reanalysis confirmed previously unsuspected disequilibrium and these samples were excluded. It might be argued that disequilibrium is more common than usually supposed.

Concentrations of thorium larger than 15 $\mu g.g^{-1}$ are rare in our sample collection. However, three widely-separated sites in Western Australia gave unusually large Th concentrations. We were initially doubtful of using these because the associated uranium analyses showed disequilibrium. However, they were considered satisfactory for the present purpose of finding the thorium concentration from pairs in the thorium chain, since these are quite independent of the U-chain and disequilibrium in the Th chain is unlikely because the lifetimes of the daughters are short on a geochemical time scale necessary to transport them in the environment. However, to fill in the upper range of concentrations, we made up artificial substandards of 15, 20, 25 and 30 $\mu g.g^{-1}$ by diluting aliquots of the New Brunswick thorium Standard NBL108 (520 $\mu g.g^{-1}$ Th) with a sediment sample measured to have 0.32 $\mu g.g^{-1}$ Th). Since NBL108 also contains a small amount of uranium, these substandards contain between 0.7 and 1.2 $\mu g.g^{-1}$ U; this is of no consequence.

Figure 1 shows a comparison of Th analyses by NAA and TSAC, the former being taken as the independent variable. In this comparison, the TSAC Th concentration is determined only by the rate of slow pairs.

The continuous straight line in the figure is an unweighted least squares fit; the equation of the fitted line and the correlation coefficient are shown. The screen efficiency used was that appropriate to each individual sample and ranged between 85 and 89%. The fitted slope is 1.03 ± 0.04 which is not significantly different from one. We consider that the agreement between NAA and TSAC is good. The dashed line corresponds to the TSAC values that would be obtained if the efficiency were assumed to be 100%. To obtain this line, the original data were reprocessed on the assumption of 100% efficiency and the data refitted. (To avoid a cluttered diagram, the data points have been omitted). The slope is 0.76 ± 0.03, which corresponds to an average efficiency of 87%. We claim that fig. 1 supports our contention that the screen efficiency is less than 100%.

"Adjusted" thorium concentrations

The estimate of thorium concentration from TSAC can be improved by making an independent measurement of uranium, say by DNA. The expected U count rate is then calculated from this value, subtracted from the total count rate and the Th concentration is then calculated from the remainder. For the reasons given earlier, this is not very important for dosimetry but it is an improvement, and is useful for comparison of TSAC with Th concentrations measured in other ways, e.g. NAA or XRS.

Figure 2 shows such a comparison of Th by TSAC/DNA with Th by NAA. The figure was constructed in the same way as fig.1. The fitted slope is 1.05 ± 0.03. This, too, is not statistically different from 1. Comparison of figs 1 and 2 shows that the correlation coefficient is increased, from 0.95 to 0.97, although both of these show that the fits are excellent. The uncertainty in the slope is reduced for the data in fig. 2.

This comparison is essentially independent of the previous one and makes no use of the pairs count. The effect of this procedure is not only to give an improved value for an individual thorium concentration but also to reduce its experimental error. This is because the estimate of thorium is now based on two data sets that are independent of the pairs count and of much greater precision. We recall that the Th concentration based on pairs is based on a relatively small number of pairs and the statistical uncertainty is commonly of the order of 15%.

It is necessary to comment on the fact that the number of data points differs in the two figures, viz: in fig. 2, the high thorium samples from Western Australia do not appear. This is because the uranium chains are in disequilibrium for these samples and DNA analysis for U cannot be used.

It may be remarked that the main reason for our introducing DNA measurements of uranium is to provide a simple and rapid check for radioactive disequilibrium. In this way we compare the concentration of the parents with the uranium concentration inferred from the alpha count rate. Since the latter is the sum of alphas from all parts of the decay chain, a discrepancy between DNA and inferred uranium usually indicates loss or gain of members of the decay chain. The thorium chain is much less likely to be in disequilibrium. Nevertheless, an independent measurement of thorium is sometimes useful, as in the present contribution.

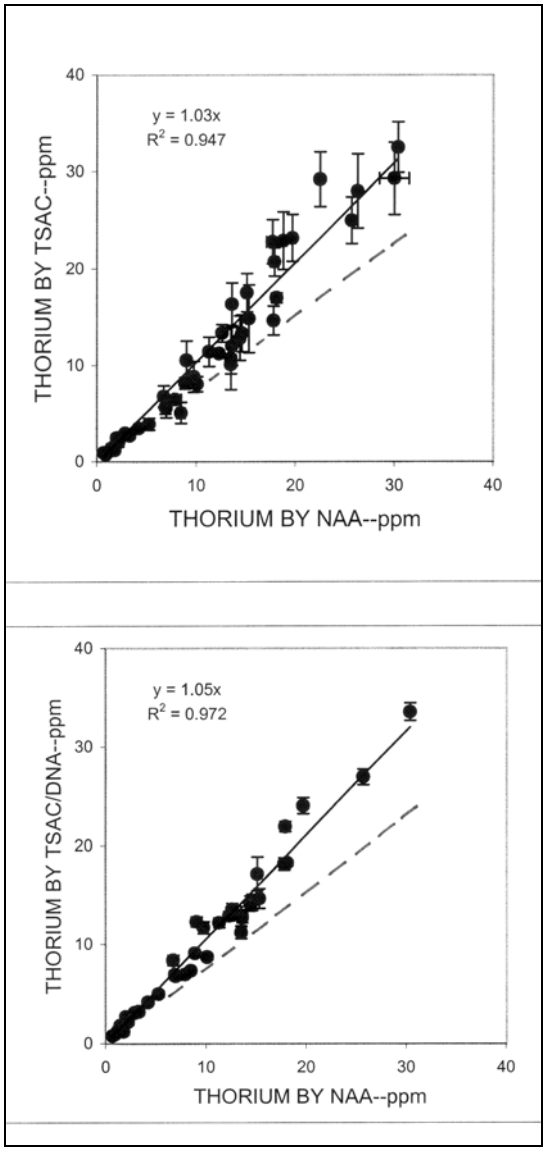

Figure 1. (upper)
Comparison of thorium concentrations found by thick source alpha counting by pairs (TSAC) and neutron activation analysis (NAA). The fitted and dashed lines are discussed in the text.

Figure 2. *(lower)*
Comparison of thorium concentrations found by thick source alpha particle counting combined with delayed neutron analysis (TSAC/DNA) and neutron activation analysis (NAA). The fitted and dashed lines are discussed in the text.

Acknowledgements

Thanks are due to D.J. Huntley for a critical reading of the manuscript. The work was supported by the Archaeometry Special Fund of the Physics Department, University of Adelaide. Shaun Cook and Dennis Rice made some of the measurements. The NAA and DNA measurements were made with grants from the Australian Institute of Nuclear Science and Engineering.

References

Adamiec, G. and Aitken M.J. 1998 Dose-rate conversion factors: update. Ancient TL, 16, 37-50.

Aitken M.J. 1985 Thermoluminescence Dating, London, Academic Press.

Aitken M.J. 1990 Pairs precision required in alpha counting. Ancient TL, 8, 12-14.

Akber R.A., Hutton J.T and Prescott J.R 1983 Thick source alpha counting using fused glass discs: correction for loss of radon and polonium. Nuclear Instruments & Methods in Physics Research A234, 394-397.

Huntley D.J., Nissen M.K., Thomson J. and Calvert S.E. 1986 An improved alpha scintillation counting method for determination of Th, U, Ra-226, Th-230 and Pa-231 excess in marine sediments. Canadian J. Earth Sci. 23, 959-966.

Jensen, H.E. & Prescott, J.R., 1983 The thick source alpha particle technique: comparison with other techniques and solutions to the problem of overcounting. Council of Europe Journal PACT 9, 25-36.

Sasidharan R., Sunta C.M. and Nambi K.S.V. 1978 TL dating: error implications in case [of] undetermined U-Th concentration ratio in pottery samples. Ancient TL No 2, 8-11.

Woithe J.M. and Prescott J.R. 1995 "Efficiencies" of phosphor screens used in thick source alpha particle counting. Ancient TL 13, No 1, 10-15.

Reviewer

D.J. Huntley

Comments

It would be much appreciated if someone would calculate new conversion factors from U and Th contents to TSAC rates, using the latest alpha particle ranges of Ziegler. The software for calculating the ranges can be downloaded from Ziegler's web site: http:/www.SRIM.org/

Authenticating marble sculpture with thermoluminescence

K. Polikreti, C. T. Michael and Y. Maniatis
Laboratory of Archaeometry, NCSR "Demokritos", Aghia Paraskevi, 153 10 Attiki, Greece

(Received 25 October 2001; in final form 25 January 2002)

Abstract: *Several attempts have been made in the past to develop a methodology for authenticating marble artifacts and monuments. They have been basically focused on understanding the weathering alterations in the chemical composition of the surface. The present study presents a new approach which concentrates on the bleaching of the thermoluminescence, occurring when the marble surface is exposed to sunlight. Exposure to sunlight reduces the TL peaks of marble to a certain low level, with similar bleaching rates for samples from different geological formations. The effect of sunlight is reduced with depth from the surface of marble. An equation-model describing the combined dependence of TL intensity on exposure time and depth from the surface of the marble is proposed. The potential of using this model as an authenticity test for artifacts continuously exposed to sunlight is proved with applications on ancient and modern pieces.*

Introduction

The need for a scientific technique to detect forgeries of marble sculpture is getting very urgent because of the continuous appearance of doubtful cases, involving large amounts of money and historical importance. The scientific community however, have not been able yet, to develop a reliable methodology. The problem arises from the fact that the bulk of a marble piece is a stable geological material and dating techniques, would give the geological rather than the historical age.

Authenticity approaches in the past, focused on the surface alterations, depositions, gradual change of ion concentration etc.

One of the most usual approaches involves testing of the disputed artefacts under ultra-violet light, where they should phosphoresce either in purple in case they are authentic, or in amber in case of forgeries (Young and Ashmole 1968). Unfortunately the results of the technique have not been scientifically documented and interpreted and consequently they are not reliable. Furthermore they depend strongly on the condition of the marble surface, past treatments (cleaning, varnishing, consolidating or even taking plaster copies).

Most researchers, on the other hand, study the gradual change of ion concentration from the surface to the marble interior (Margolis and Showers 1988, Ulens et al. 1995). However, these changes are not easily quantifiable due to their complicated formation procedures and unfortunately they can be produced artificially in the laboratory (Heller and Herz 1995). Furthermore, the reports on gradual ion transportation inwards and outwards from the bulk of marble, have not been verified on ancient samples.

The present work intends to contribute in the authenticity of marble from another point of view. Our approach concentrates on the defects existing in the marble since geological times. Exposure to sunlight anneals these defects up to a depth depending on the exposure time. The technique of Thermoluminescense is used to quantify the relationship between depth and exposure time and an equation model is proposed, which discriminates ancient from modern surfaces exposed to sunlight for a considerable period of time.

The results presented here are a first step towards the development of a new full methodology for solving authenticity problems of marble artefacts under all conditions.

Experimental methods and techniques

All the thermoluminescence measurements were performed by using the aluminum foil technique (Michael et al. 1997, Michael et al. 1999). The powdered sample is spread with a small paint brush on aluminium foil discs (diameter of 1cm, thickness of 8μm) and covered by silicon grease. The technique ensures good heating contact between sample and heater plate and increases reproducibility even in high heating rates. Another advantage is the reduction of chemiluminescence, since the measurements can be performed under vacuum. The heating rate was 14°C/sec and a BG39 (infrared absorption filter) was used. Normalisation of the peaks was made by dividing with a monitor beta dose (^{90}Sr: 0.52 gray/min).

The effects of mechanical treatment (Wintle 1975, Goksu et al. 1988) have been proved to be disastrous in calcite dating and several remedies have been proposed (Wintle 1975, Bangert and Henning 1979), the pressure exerted is the main cause (Maniatis and Mandi 1992). In order to avoid tribo-luminescence (in this case new traps created on the grain surfaces by grinding), the powdered samples were etched with acetic acid 0.5% for 1 min.

Maximum reproducibility of the peak intensities was achieved for grain sizes between 80 and 125μm and this range was used in sample preparation. The reproducibility of the peak temperature was calculated at ±1°C and of peak intensity at 22%.

All measurements and sample preparations were performed under red light. The use of a solar simulator was avoided since several researchers report that the presence in the light source of a strong ultraviolet component gives risk of removal of residual TL or phototrasfer phenomena (Aitken 1985, McKeever 1986). All samples thus were exposed to natural sunlight, in June, October and November in Athens.

The specimens for the TL profile measurements were cylinders of diameter 20mm and length 60mm approximately, drilled out in red light. After cleaning them with HCl, 0.5 N they were exposed to natural sunlight. Following that, thin (1-1.5mm) slices parallel to the exposed surface were cut from the surface to the interior of the specimens and cleaned again with HCl, 0.5N.

Results and Discussion

The natural thermoluminescence of marble was studied on thirty four samples from fifteen different quarries, with various Mn^{2+} concentrations and grain sizes. Mn^{2+} is considered the main recombination center for calcites (Medlin 1968, Lapraz and Iacconi 1976, Calderon et al. 1984, Down et al. 1985). Typical glow curves of marble are given in Figure 1. Three peaks are generally observed in agreement with other researchers (Bruce et al. 1999) and their energy depths were measured with the initial rise method and peak shift with heating rate (Mc Keever 1985): a) A peak produced by photo-transferred thermoluminescence (Lima et al. 1990, Liritzis et al. 1996, Bruce et al. 1999) at around 180°C, b) a well defined and stable peak at 285-300°C (lifetimes from 10^5 to 10^8 years) and c) a very stable (lifetimes from 10^7 to 10^{12} years) peak, of low intensity at 325-390°C, which overlaps with black body radiation. This peak has been used for calcite dating in the past (Wintle 1978, Debenham and Aitken 1984). However, our experiments showed that the peak at 290°C is quite suitable for monitoring the changes of thermoluminescence of marble due to bleaching and as it is better defined than the 325-390°C peak was used in this work.

The relative intensities between the two high temperature peaks vary for different types of marble. The ratio observed in curve 1a corresponding to Naxian marble is the most common one.

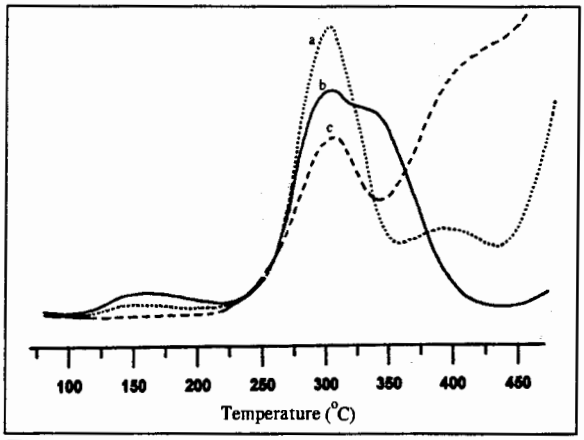

Figure 1.
Typical thermoluminescence curves for different types of marble:

a) White Naxian (Apollon quarry) (intensity multiplied by 5)
b) White Pentelic
c) White Thassian (Aliki quarry) (intensity multiplied by 5).

Bleaching of thermoluminescence was observed in all types of marble exposed to sunlight. Marble slabs (4x4 cm^2, 4 mm thickness), were exposed to sunlight for different time intervals. The resulting plot for the peak at 290°C is shown in Figure 2 (Parian marble, Lychnites). The experiment was repeated with samples from four different quarries with different grain sizes and Mn^{2+} concentration. The peak at 290°C, shows the same behaviour in all quarry samples: After 20 minutes of exposure, the peak loses 80% of its initial intensity. The reduction in peak intensity continues at a lower rate, until 60min when it reaches the lowest level which remains practically constant even after a prolonged exposure (residual TL) say 3 months. The intensity of the residual level is usually 11 to 18% of the natural thermoluminescence.

The data in all cases can be fitted by the sum of two exponential functions (Polikreti et al. 1996, Liritzis et al. 1996). One with a time constant of 0.09-0.16 min^{-1} and a second one with a time constant of 0.001-0.002 min^{-1}(Table 1). The phenomenon can be explained by the existence of two different types of electron traps in the $CaCO_3$ lattice. Electrons in these

traps have different escape probabilities. Those with the higher probabilities of escape are evicted from their traps easily and cause the high bleaching rate observed at the first 20 minutes.

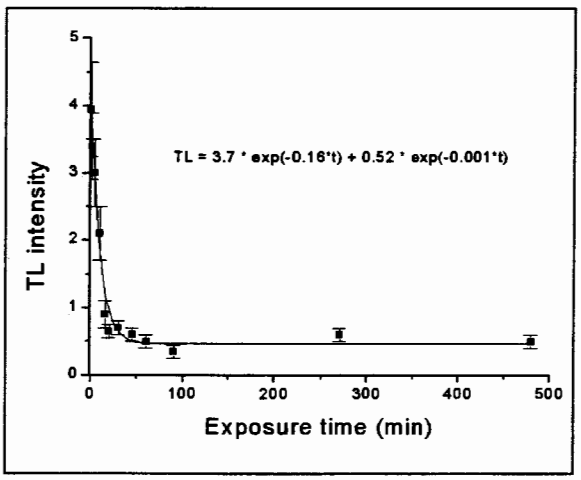

Figure 2.
TL intensity versus exposure time (white Parian marble, Lychnites). TL intensities are normalised with a second glow.

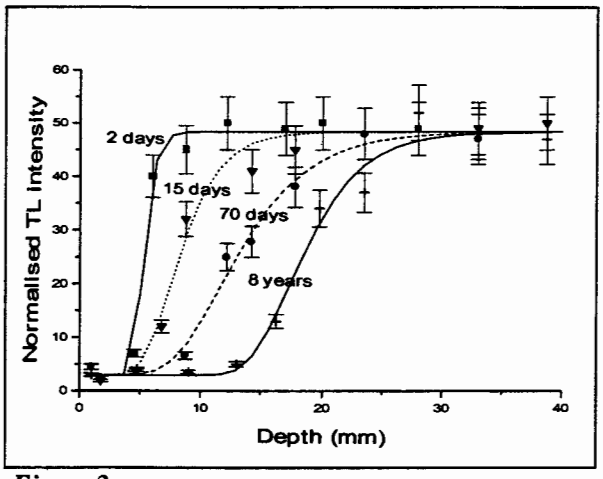

Figure 3.
Thermoluminescence versus distance from the marble surface for various exposure times (Pentelic marble). TL intensities are normalised with the second glow.

For a detailed study of thermoluminescence versus distance from the surface, the TL profiles of thermoluminescence with depth were drawn for three specimens from a quarry from Pentelikon mountain. They were exposed to natural sunlight for 2, 15 and 70 days (Fig. 3). Another profile, of a surface exposed for 8 years (the date of last use of a modern marble quarry) was also drawn. All curves show an initial part near the exposed surface where thermoluminescence is minimum and then an almost linear increase, up to a maximum value which corresponds to the natural (geological) thermoluminescence of the particular marble piece.

In an attempt to find an equation describing the curves of Figure 3, the following assumptions were adopted:

Theoretical Approach

To simplify the calculations, we assume that the decrease of TL versus time is represented by an exponential term plus a constant. This simplification does not introduce major errors since the second exponential term fades very slowly (Tab. 1). According to this assumption TL at two different depths d and d+x, which correspond to exposure times t_d and t_{d+x} will be:

$$TL_d = R + C \exp(-\lambda_d t_d) \quad (a)$$

$$TL_{d+x} = R + C \exp(-\lambda_{d+x} t_{d+x}) \quad (b) \qquad (1)$$

where R is the the residual TL, C the geological minus residual TL and λ_d the time constant at depth d If the two TL intensities are equal, then:

$$\lambda_d t_d = \lambda_{d+x} t_{d+x} \qquad (2)$$

Now we can assume that the marble matrix, is an homogenous and isotropic material, where the intensity of a light beam passing through it, decreases according to Lambert - Beer law:

$$I_{d+x} = I_d \exp(-kx) \qquad (3)$$

where I_d, I_{d+x} are the beam intensities at depths d and d+x and k(mm^{-1}) is a constant depending on the wavelength of sunlight radiation and the transparency of marble (i.e. density, texture, grain size and accessory minerals).

Assuming that the total number of sunlight photons or the total energy E (=I·S·t), needed to decrease natural TL to a certain intensity is the same for the two depths d and d+x, we have:

$$E = I_{d+x} \cdot S \cdot t_{d+x} = I_d \cdot S \cdot t_d$$

where S is the cross-sectional area.

Hence from eq. 3,

$$t_d / t_{d+x} = \exp(-kx) \qquad (4)$$

and combining with eq. (2) we have:

$$\lambda_{d+x} = \lambda_d \exp(-kx) \quad (5)$$

Introducing eq. 5 to eq. 1(b) gives (for d=0) a double exponential equation:

$$TL_x = R + C \exp(-\lambda_o t \exp(-kx)) \quad (6)$$

where λ_o (day^{-1}) is the time constant for the TL exponential decay versus exposure time at the marble surface.

Application on the experimental data

Equation (6) was used as a fitting function on the experimental data of the TL profiles with depth, for 2, 15, 70 days and 8 years (Fig. 3). Average values for R (2.9 r.u.) and C (45.5 r.u.) were calculated from the data. The fitting seems satisfactory, however the calculated constants k and λ_o (Tab. 2), appear to decrease with increasing exposure time (although the λ_o errors are very large).

This behavior indicates that the equations describing the phenomenon are much more complicated than assumed. The coefficient k for example, depends actually on wavelength, a fact that could introduce an error, given that marble absorbs strongly at the ultraviolet region (Vaz et al. 1968), which is also the critical region for TL bleaching. On the other hand, calcite crystals show decreased optical absorption after they have been subjected to ultraviolet irradiation (Vaz et al. 1968). These data agree with our experimental results showing that k decreases with exposure time.

As for the time constant λ_o, it is expected to decrease for longer exposure times, since the average solar radiation intensity in 100 years is smaller than that of 70 days of sunny weather, due to weather variations. However, taking meteorological data into account, i.e., multiplying the exposure time by a factor representing the mean solar radiation intensity for the particular period the experiment took place, introduces very small corrections, which give results within the experimental errors. The large errors for λ_o, could be reduced if we increase the number of experimental points in the linear part of eq. 6. For technical reasons, it was not possible to have more than 2-3 slabs every 3-5 mm, at this first stage.

Time-Depth model for authenticity testing

In order to avoid the problems occuring due to the variations of k and λ_o, without loosing the correlation of the phenomenon with time, the inflection point of the double exponential function was found:

$$t = (1/\lambda_o) \exp(kx_{ip}) \quad (8)$$

where x_{ip} is the inflection point, in which the TL is calculated: TL= R + C/e.

Equation (8), from now on refered to as "time-depth model", can be used to calculate the exposure time for a certain measured depth x_{ip}, by using "effective" values of k and λ_o, characteristic for each type of marble. These values can be calculated from fitting with equation (8) at least three experimental (t, x_{ip}) pairs.

The model can be used as an authenticity test according to the following procedure: Three TL profiles are drawn, corresponding to specimens exposed for known times. The x_{ip} depths are estimated for each profile, with the use of the double exponential function (Eq. 6). Fitting the (t, x_{ip}) pairs by the time-depth model (eq. 8), gives "effective" values for k and λ_o. Then an unknown exposure time can be calculated by measuring the corresponding x_{ip} depth. This can be done for every piece of the same marble type.

For Pentelic marble, the effective values of k and λ_o calculated by treating the data of Figure 3 as described above are: k = 0.67 (±0.02)mm^{-1} and λ_o = 53 (±15)day^{-1}.

Figure 4 shows the behaviour of depth x_{ip} with exposure time. The effective values lie within the range calculated from the fitting by the double exponential (Table 1).

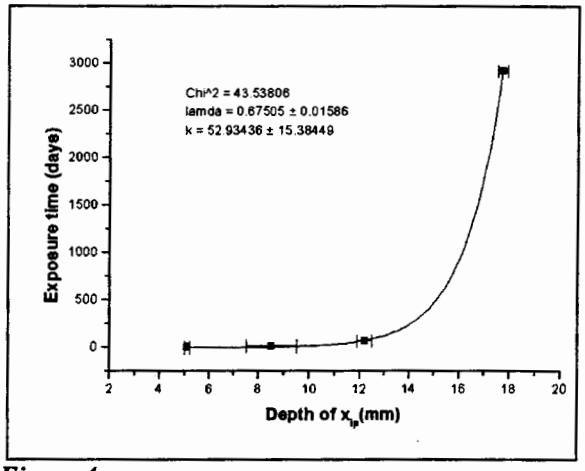

Figure 4.
Time - Depth model for Pentelic marble (x_{ip} is the inflection point of eq. (6), lamda and k as in eq. (8))

For another type of marble, different effective values are expected for k and λ_o, as they depend on marble transparency and solar radiation intensity. For a Venetian piece of marble identified as Naxian (Polikreti and Maniatis 2001) for example, effective values of k and λ_o are: k = 1.021 (±0.002)mm^{-1} and λ_o = 9.8 (±0.3)day^{-1}. The resulting larger k value is in agreement with the lower transparency of Naxian marble compared to that of Penteli.

Table 3 shows some depths of x_{ip}, for typical exposure times calculated by eq(8), for Pentelic and Naxian marbles. This table shows the potential of the method as an authenticity test and approximate dating method. According to Table 3, the method gives broad age ranges for marble objects exposed to sunlight. For example, an object made of Pentelic marble with a x_{ip} depth calculated at 24 mm, is given an age of 300 to 1000 years (1000-1700 AD). The range resulted by assuming an error for x_{ip} equal to 1mm, which is the maximum error value calculated in all studied cases (Tab. 2). Similar ranges can be assigned to objects made of Naxian marble.

In order to evaluate the efficiency of the proposed model in actual problems, we attempted to "date" a small, worked parallelepiped block abandoned in an ancient quarry and a modern quarry front, both from Pentelikon mountain. The piece bears toolmarks (point chisel), securely identified as "ancient". The modern front shows an almost white surface, with traces of loose depositions.

The inflection points for the ancient and the modern profiles (Fig. 5a and b) were calculated at $x_{ancient}$ = 25.0 (±0.5) mm and x_{modern} = 20.50 (±0.05) mm. These depths, according to the model correspond to $t_{ancient}$ =1103 (±656) years (300-1500 AD) and t_{modern} = 53 (±23) (errors calculated by propagation of errors procedure). The results confirm that the proposed methodology can easily distinguish ancient from modern marble surfaces, exposed to sunlight for long periods.

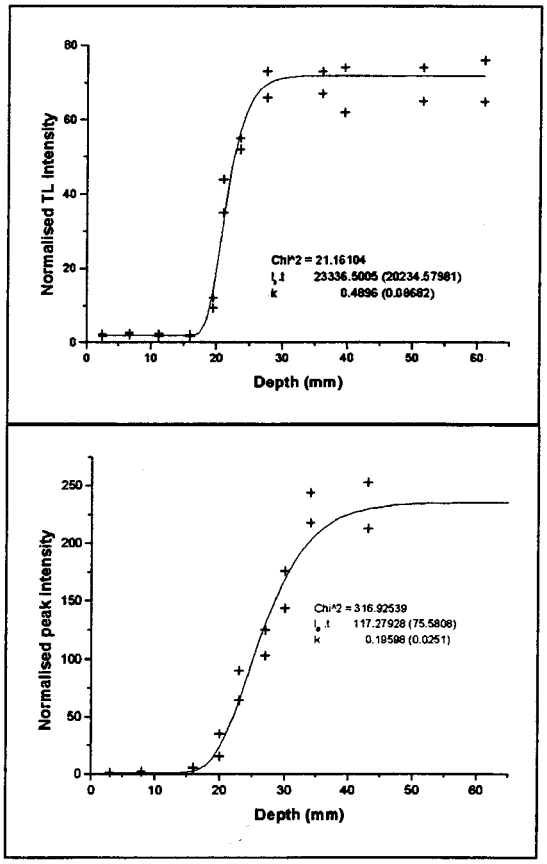

Figure 5.
TL profiles for two Pentelic marble surfaces (intensities normalised with a second glow, λ_o.t and k as in eq. (6)):
a) a piece bearing ancient toolmarks (x_{ip} = 25mm) and
b) a modern quarry front (x_{ip} = 20.5mm)

Conclusions

The natural thermoluminescence of marble and the effects of natural sunlight irradiation on the surface of ancient marble monuments were studied. Bleaching rates and dependence of thermoluminescence on depth were calculated for different types of marble.

The results lead to a time-depth model for samples continuously exposed to sunlight. This model is still in a preliminary form but it could lead to a method for testing the authenticity of disputable marble monuments. In its initial form it can distinguish between samples exposed to sunlight recently from those exposed since antiquity. If the studied marble piece is homogenous and the sources of error are minimised, the method can give a really narrow age range.

Table 1.
Maximum Grain Size (MGS), Mn^{2+} concentration (in relative units, measured by EPR spectroscopy), residual TL and fitting function of the TL decrease versus time, for different types of marble.

Sample description	Mn^{2+} (r.u.)	MGS (mm)	Residual TL (% of natural)	Fitting function
White, Pentelic	2012	0.6	14	$1.90\,e^{-0.10x} + 0.37\,e^{-0.001x}$
Whitish, Naxian	860	3.0	18	$0.80\,e^{-0.14x} + 0.40\,e^{-0.001x}$
White, Parian	184	1.0	14	$3.7\,e^{-0.16x} + 0.52\,e^{-0.001x}$
White, Thassian, dolomitic	685	1.6	11	$10.10\,e^{-0.09x} + 2.6\,e^{-0.002x}$

Table 2.
λ_o and k calculated by eq. (6) and inflection points by eq. (8) (Pentelic marble).

Exposure time (days)	λ_o ($days^{-1}$)	k (mm^{-1})	x_{ip} (mm)
2	1816 ± 4611	1.6 ± 0.5	5.1 ± 0.1
15	2 ± 2	0.4 ± 0.2	9 ± 1
70	0.3 ± 0.2	0.25 ± 0.05	12.2 ± 0.3
8x365	0.1 ± 0.1	0.31 ± 0.08	17.7 ± 0.2

Table 3.
The x_{ip} depth calculated by the time–depth model for typical exposure times.

Exposure time (years)	x_{ip} *for Penteli (mm)*	x_{ip} *for Naxos (mm)*
10	18.1	10.3
100	21.0	12.5
500	23.8	14.1
1000	24.8	14.8
2000	25.9	15.4
3000	26.5	15.8
5000	27.2	16.4

It is a first time that bleaching of defects in marble by the sunlight as a function of time and depth was studied in detail. The results are leading to the development of an authenticity test for ancient marble artefacts that gives reproducible numeric results, close to the real ages. The model has, of course, to be improved in order to include artefacts exposed to sunlight and then buried for long periods. This will take into account the expected increase in TL intensity due to the natural irradiation from the radioactive elements of the ground, a standard procedure in TL dating. This modification will extend the application to complicated exposure histories such as exposure, burial and exposure to sunlight again. These natural processes are very difficult to be reproduced by forgers.

References

Aitken, M. J. (1985) *Thermoluminescence Dating*. Academic Press. London.

Bangert, U. and Henning, G. J. (1979) Effects of sample preparation and the influence of clay impurities on the TL-dating of calcite cave deposits. *PACT* **3**, 281-289.

Bruce, J., Galloway, R. B., Harper, K. and Spink, E. (1999) Bleaching and Phototransfer of thermoluminescence in limestone. Radiat. Meas. **30**(4), 497-504.

Calderon, T., Aguilar, M., Jaque, F. and Coy-yll, R. (1984) TL from natural calcites. *J. Phys. C: Solid State Phys.* **17**, 2027-2038.

Debenham, N. C. and Aitken, M., J. (1984) TL dating of stalagmitic calcite. *Archaeometry* **26**(2), 155-170.

Down, J. S., Flower, R., Strain, J. A. and Townsend, P. D. (1985) TL emission spectra of calcite and iceland spar. *Nucl. Tracks Radiat. Meas.* **10**(4-6), 581-589.

Goksu, H. Y., Pennycock, S. J. and Brown, L. M. (1988) TL and CL studies of calcite and MgO: Surface defects and heat treatment. *Int. J. Radiat. Appl. Instrum., Part D, Nucl. Tracks Radiat. Meas.* **14**(3), 365-368.

Heller, D. S. and Herz, N. (1995) Weathering of dolomitic marble and the role of oxalates, Analytical methods useful in authenticating ancient marble sculptures. *Transac. 3rd Intern. Symp. of the Assoc. for the Study of Marble and Other Stones used in Antiquity (ASMOSIA)*, Archetype, London, Maniatis, Y., Herz, N. and Bassiakos, Y. (eds.), 167-276.

Lapraz, D. and Iacconi, P. (1976) On some luminescent and optical properties of synthetic calcite single crystals. *Phys. Status Solidi (A)* **36**, 603-615.

Lima, J. F., Trzesniak, P., Yoshimura, E. M. and Okuno, E. (1990) Phototransferred thermoluminescence in calcite. *Radiat. Prot. Dosim.* **33**, 1/4, 143-146.

Liritzis, I., Guibert, P., Foti, F. and Schvoerer, M. (1996) Solar bleaching of thermoluminescence of calcites. *Nucl. Instrum. Meth.* (B) **117**, 260-268.

Liritzis, I. and Bakopoulos Y. (1997) Functional behaviour of solar bleached thermoluminescence in calcites. *Nucl. Instrum. Meth.* (B) **132**, 87-92.

Maniatis Y. and Mandi V. (1992) Electron Paramagnetic Resonance Signals and Effects in Marble Induced by Working. *J. Appl. Phys.* **71**, (10), 4859-4867.

Margolis, S. V. and Showers, W. (1988) Weathering characteristics, age and provenance determinations on Ancient Greek and Roman artefacts. *Classical Marble: Geochemical, Technology, Trade*, Herz N. and Waelkens M. (eds.), 233-242.

Medlin, D. R. (1968) The nature of traps and emission centers in TL rock materials. *Thermoluminescence of Geological Materials*, McDougal D. J. (ed.), Academic Press, London, 193-223.

McKeever, S. W. S. (1985) *Thermoluminescence of solids*, Cambridge University Press, Cambridge.

Michael, C. T, Zacharias, N., Polikreti, K. and Pagonis, V. (1999) Minimising the spurious TL of recently fired ceramics using the foil technique. *Radiat. Prot. Dosim.* **84**(1-4), 499-502.

Michael, C. T., Zacharias, N., Maniatis, Y. and Dimotikali, D. (1997) A new technique (foil technique) for measuring natural dose in TL dating and its application in the dating of a mortar containing ceramic fragments. *Ancient TL* **15**(2-3), 36-42.

Polikreti, K., Michael, C. T. and Maniatis, Y. (2001) Study of the effects of environmental radiation on marble surfaces by Thermoluminescence: Application on the authentication of ancient artifacts. *Proc. 3rd Symp. Hellenic Soc. of Archaeometry*, 6-9 November 1996, Bassiakos Y., Aloupi E. and Facorellis G. (eds), 47-55.

Polikreti, K. and Maniatis, Y. (2002) A new methodology for marble provenance based on EPR spectroscopy. *Archaeometry*, **44**, 1-21.

Ulens, K., Moens, L. and Dams, R. (1995) Analytical methods useful in authenticating ancient marble sculptures, *Transac. 3rd Intern. Symp. Assoc. for the Study of Marble and Other Stones used in Antiquity (ASMOSIA)*, Archetype, London,

Maniatis, Y., Herz, N. and Bassiakos, Y. (eds.), 199-205.

Vaz, J. E., Kemmey, P. J. and Levy, P. W. (1968) The effects of ultraviolet light illumination on the thermoluminescence of calcite. *TL of geological materials*, McDougal D. J. (ed.), Academic Press, London, 111-125.

Wintle, A. G. (1975) Effects of sample preparation on the TL characteristics of calcite. *Modern* Geol. **5**, 165-167.

Wintle, A. G. (1978) A thermoluminescence dating study of some Quaternary calcite: potential and problems. *Can. J. Earth* Sci. **15**, 1977-1986.

Young, W. J. and Ashmole, B. (1968) The Boston relief and the Ludovici Throne. *Boston Museum of Fine Arts Bulletin* **66**, 124-166.

Reviewer

G. Wagner

Color images of infrared stimulated luminescence (IRSL) from granite slices exposed to radiations

Tetsuo Hashimoto*, Hayato Usuda, and Takashi Yawata****
*Department of chemistry, Faculty of Science, and **Graduate School of Science and Technology, Niigata University, Ikarashi-ninocho, Niigata, 950-21, Japan

(Received 19 June 2002)

Abstract: *Color luminescence images, associated with stimulation by infrared light, were obtained from some granite slices after X-ray irradiation of 200 Gy. The infrared stimulated luminescence color images (abbreviated to IRSL-CI) showed two colors, separable into intense yellow and blue portions. The former was assigned to be originated from a plagioclase feldspar constituent and the latter to potassium feldspar one. Quartz parts scarcely gave distinct IRSL-pattern. From spectrometry of the IRSL, two main emission peaks, consisting of 550 nm (yellow) and 580 nm (orange), were revealed besides moderate emission in wavelengths shorter than 450 nm (blue). Unexpectedly, reddish IRSL was observed in white mineral, probably feldspar of one granite. This IRSL-CI method can be useful for the examination of feldspar purity as well as for the filter selection of IRSL-dating.*

Introduction

In the optical dating method, Hütt et al., (1988) have discovered the infrared-stimulated luminescence (IRSL) phenomena for most of feldspars; when ionizing radiation-exposed feldspars were stimulated with infrared light in the range of 800-900nm, the strong IRSL has been detected in the wider wavelength range including almost visible light. According to a review paper by Krbetschek et al., (1997), various kinds of luminescence windows in wavelengths were reported to the IRSL of feldspar. In our laboratory, some luminescence color imaging methods, including thermoluminescence color images (TLCI), afterglow color images (AGCI), photo-induced phosphorescence (PIP), color center images (CCI) and 2-dimensional monochromatic OSL-images, have been established using varieties of granite slices (Hashimoto et al., 1995). Subsequently, the color imaging methods of radiation-induced luminescence have been applied to 16 kinds of feldspar minerals on the basis of a ternary diagram of feldspar. As a result, the AGCI could be separated into two groups, giving intensely bluish or green coloration along the alkali feldspar line and weak reddish coloration along the plagioclase line. In most feldspar slices, heterogeneous color distribution has been revealed according to the mineral formation and historical conditions (Hashimoto et al., 2001).

Since the IRSL of feldspar is much effectively bleached at deposition (Aitken, 1998), the IRSL-dating of feldspars has been expected to be more hopeful for the widespread quaternary-sediment layers, applicable to complete bleaching effects with the sunlight. In the IRSL-measurements, the selection of filter-combination is very important to choice the objective feldspar suitable for dating with low background conditions as well as for checking the purification of feldspar samples.

From these situations, a simple IRSL-color imaging method from granite slices has been developed using a high sensitive photographic system accompanied with combination of color filters. In the 2-dimensional color images, mainly yellowish and slightly bluish IRSL parts have been recognized as well as with heterogeneous distribution on every sample exposed with a γ-ray standard source.

Experimental

1. Preparation of granite slice samples

The following granites were selected to prepare the slice samples in the 2-dimensional color images described below; A) HW-5 granite, mylonite-like sub-facies (granodiorite), B) HW-36 granite, porphyritic sub-facies (granodiorite) and C) HW-23 granite, foliated granodiorite-tonalite facies. All of the HW granite samples were collected from Hanawa pluton adjacent to Tanakura Shear Zone, by which the main fault divided North-eastern Japan from Southwestern Japan during the Mesozoic period (Ohira, 1992, 1994).

After cutting roughly into square planes (approximately 8x8x0.5 mm), each surface was polished with an alumina emulsion solution. Every sliced rock sample was followed by the X-ray irradiation.

2.Radiation exposure and observation of IRSL-color

images

All luminescence color images were observed after the irradiation of X-rays using a fluorescent X-ray analysis apparatus (SX3063p, Rigakudenki Co. Ltd.) and a ^{137}Cs standard γ-ray source (Pony Co. Ltd., PS-3000 SB Type) for the dose standardization. Following X-ray irradiation with the absorbed dose of 200Gy (for 15min exposure time), slice samples were stored to eliminate completely afterglow emission, by letting the samples stand for 1 day in a dark box. The IRSL-color imaging (IRSL-CI) observation of the slice samples was carried out by means of a photographic apparatus as illustrated in Fig. 1(a). Infrared light emitting diode (IR-LED, Hamamatsu Photonics, L2690-02) is certified to offer 890 nm emission peak with 50 nm FWHM value. Sixteen LEDs were installed to a LED holder having a hole of 20 mm in diameter and the applied current was fixed here to 100mA per LED. The applied IR-power was evaluated to be 3.0 mW/cm^2 on the surface of the slice samples using a power meter. For the IRSL-CI photography, a glass filter (Asahi-techno Glass Co. Ltd., CF-50E) for correction in visible light was inserted to eliminate the stimulation IR-light. The optical properties of the filter and stimulation light-ranges from IR-LED are indicated in Fig. 1(b). To attain most sensitive photography, a camera (Nikon, F-3) with a lens of F-1.2 was employed as well as the use of highly sensitive color film (Fuji ISO-400). The practical photography has been conducted in a dark room and the camera shutter was opened for 90 sec from start of the IR-LED stimulation.

3. IRSL-spectrometry by an on-line spectrometric system

An on-line spectrometric system for extremely weak photon-emission was applied to the spectrometry of IRSL from the granite slices in the similar way to the TL-spectrometry (Hashimoto et al., 1997). Instead of the camera, a small spectrometer, connected to image intensified photo-diode array, was placed in the same arrangement as shown in Fig. 1(a). Every scanning interval was 22 ms and 512 channel data in wavelength width were summed up to 45 cycles to form one spectrum per second. Thus, 100 spectra during the period of 100 sec stimulated with IR-light, could be acquired to the microcomputer memory. All of the spectrum data were plotted in a spectrum figure for every slice sample.

Results and discussion

Infrared-stimulated luminescence color images (IRSL-CIs) of some X- irradiated granite slices were obtained using photon detection are shown in Fig. 2.

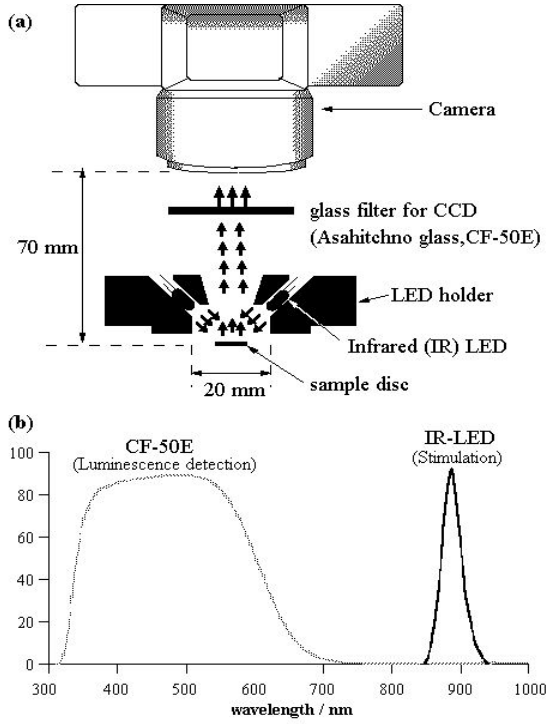

Figure 1.
Schematic view of photographic assembly for infrared stimulated luminescence color imaging (IRSL-CI) from slices exposed radiation (a) and optical properties of IR-LED and a IR-cut filter (CF-50E).

The present results from IRSL-CIs show evidently that feldspar portions in the real images tend to cause strong yellowish luminescence, while quartz portions bring on no IRSL-CI because of extremely weak luminescence emission with IR-illumination. In addition to scattered distribution of the IRSL-images, there appears heterogeneous distribution on the IRSL-CIs within single feldspar grain part. The similarly heterogeneous distribution of afterglow and thermoluminescence was observed within every single feldspar slice (Hashimoto et al., 2001).

In the preceding publication (Hashimoto et al., 1995), it has been recognized that among several kinds of white mineral constituents in granite, albite, plagioclase and potassium feldspars are sensitive to the radiation-induced luminescence, involving radio-luminescence (RL), TL, afterglow, photo-induced phosphorescence as 2-D color images. On the other hand, quartz constituent shown relatively poor sensitivity to luminescence phenomena. The present results are in good agreement with the highest sensitivity natures of plagioclase portions in any kinds of the luminescence (Hashimoto et al., 1995, 2001).

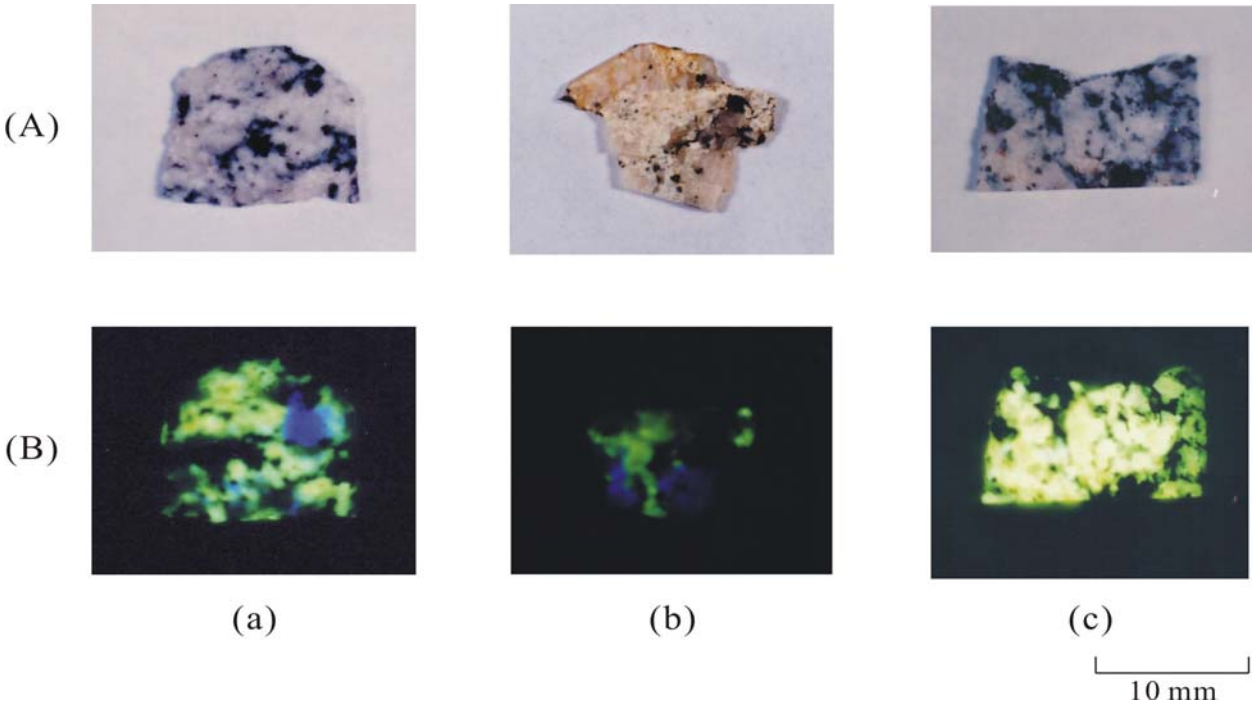

Figure 2.
Typical infrared stimulated luminescence color images (IRSL-CIs) from granite slices. Real surface images (A) and IRSL-CI (B) were obtained from three kinds of granite slices; (a) HW-5, (b) HW-36, and (c) HW-23.

Additionally, it is well known that light-sensitive trapped electrons (and hole centers) in minerals should be greatly dependent on the kinds of minerals in which they are located, as well as the geological history of the rock body formation (Hashimoto et al., 1994). From this viewpoint, the IRSL-CIs themselves were considered to reflect such mineral properties. However, there appears no significantly different pattern among the present slices, except for two samples, HW-5 and HW-36, which show the mixture images distinguishable into yellow and blue part, while HW-23 sample renders intense yellowish patterns alone. The HW-23 sample is known to contain almost plagioclase constituent as feldspar, so that the intense yellow IRSL-CI portions are attributable to plagioclase mineral. Two other granites, HW-5 and HW-36 have been analyzed to contain small parts of potassium feldspar constituent in addition to large amount of plagioclase portions according to Ohira, (1994). Therefore, the blue IRSL-CI portions seen in HW-5 and HW-36 were assumed to originate from potassium constituents. In fact, single potassium feldspar gave blue luminescence color in both afterglow and thermoluminescence. The identification of plagioclase and potassium feldspar portions was also confirmed by a mineralogist. Anyway, it should be emphasized that IRSL-color images in Fig. 2 are the first visualization, by which the researchers could admit simply the IRSL-CIs, helpful for the selection of IRSL-detection filter, superior to the monochromatic IRSL-images from our laboratory (Hashimoto et al., 1995).

In further precise way, the results from an IRSL-spectrometry could serve for the determination of detection wavelength range, although the two-dimensional information couldn't be obtained. Spectral results from three granite slice samples are presented in Fig. 3.

Every highest spectrum is corresponding to first IRSL just after beginning of IR-LED illumination because of decaying behavior of IRSL as well known. In the HW-5 sample, there exists a prominent yellowish emission having a peak at 550 nm. In addition to 550 nm peak (yellow color), there appears another 580 nm (orange color) peak and other emission in shorter wavelength than 450 nm ranges (blue or violet color) in two granites, HW-36 and HW-23. Among these luminescence wavelength ranges, yellow and orange colors tend to decay out immediately after the IR-illumination, whereas the blue or violet emission continues for a relatively long period. This result will support also the two different minerals for IRSL-emission, probably plagioclase

and

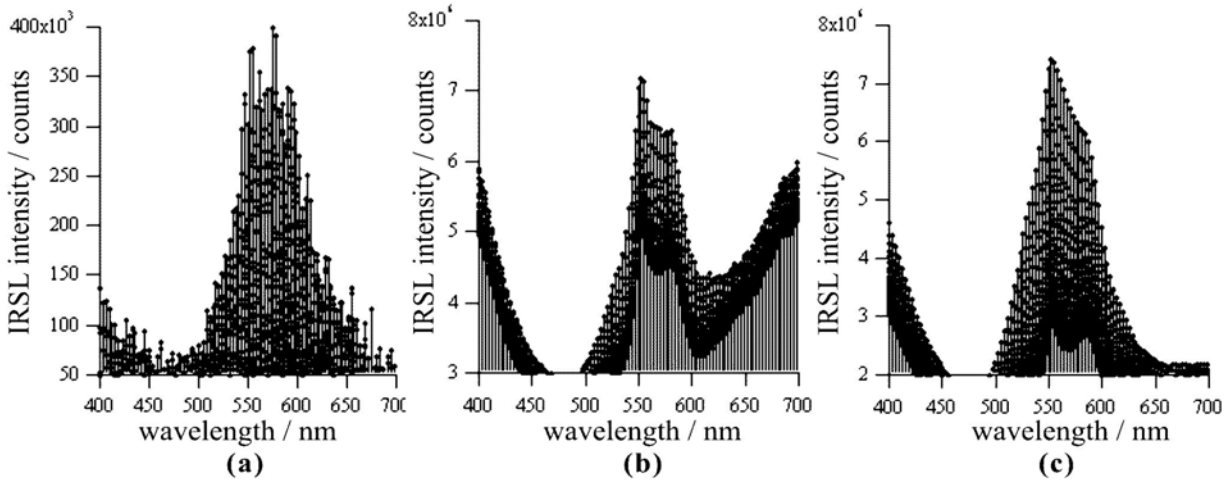

Figure 3.
IRSL-spectra measured by an on-line spectrometry installed with an image intensifier. Every spectrum is consisting of 100 spectra dependent on decaying behavior after IR-LED-illumination. Granite samples are (a) HW-5, (b) HW-36, and (c) HW-23

potassium feldspars in these granite slices.

It is noteworthy that the spectra (b) from HW-36 offer the existence of longer wavelength side beyond 600 nm, corresponding to reddish color ranges. In a preceding paper (Hashimoto et al., 1995), the similarly originated granite showed reddish PIP (photon-induced-phosphorescence) pattern (HW-38). Although the IRSL-spectrum shows certainly reddish emission, it must be questionable that there appears no red part on the IRSL color image of HW-36 (Fig. 2(b)). The reason should be attributable to the use of IR-cut filter (CF-50E) as indicated optical property in Fig. 1(b), in which the reddish wavelength ranges were almost completely absorbed (c.f. emission spectrum in Fig. 3(b)).

Similar color images of the IRSL will be realized using highly sensitive CCD-camera in near future. To approach this direction, we are starting the color imaging visualization and decay curve analysis into red, green and blue coloration of the imaging data.

Since the PIP-phenomena should be derived from the same photon-sensitive trapped electrons, the PIP-color images might be displaced to the IRSL-color photography in the case of weak IRSL-emitting minerals.

These IRSL-CI technique must be useful for the examination of feldspar purity and the filter selection for the establishment of the reliable IRSL-dating, together with emission spectrum data.

Acknowledgements

The authors are grateful to Prof. T. Toyoshima of our university for useful information of mineral (feldspars) identification on slice samples. The present work was supported greatly by Grant-in Aids for Fundamental Science Research from the Ministry of Education, Science, Culture and Sports, Japan (No. 14340231).

References

Aitken, M. J.. (1998). An Introduction to Optical Dating: The dating of quaternary sediments by the use of photo-stimulated luminescence. Oxford University Press, Oxford.

Hashimoto, T., Sakaue, S., Ichino, M., Aoki, H., (1994). Dependence of TL-property changes of natural quartzes on aluminium contents accompanied by thermal annealing treatment. *Nucl. Tracks Radiat. Meas.*, **23**, 293-299.

Hashimoto, T., Notoya, S., Ojima, T., Hoteida, M., (1995). Optically stimulated luminescence (OSL) and some other luminescence images. *Nucl. Tracks Radiat. Meas.*, **24**, 227-237.

Hashimoto, T., Sugai, N., Sakaue, H., Yasuda, K., Shirai, N., (1997). Thermoluminescence (TL) spectra from quartz grains using on-line TL-spectrometric system. *Geochem. J.*, **31**, 189-201.

Hashimoto, T., Yamazaki, K., Morimoto, T., Sakaue, H., (2001). Radiation-induced luminescence color images from some feldspars *Anal. Sci.*, **17**, 825-831.

Hütt, G., Jack, I., Tchonka, J., (1988). Optical dating: K-feldspars optical response stimulation spectra. *Quatern. Sci. Rev*., **7**, 381-385.

Krbetschek, M. R., Goeze, J., Dietrich A., Trautmann T., (1997). Spectral information from minerals relevant for luminescence dating. *Radiat. Meas*., **27**, 695-748.

Ohira, H., (1992). Genetic relation between magmatic differentiation and morphology of zircon of the Hanawa pluton. *J. Mineralogy, Petrology & Economic Geol*., **87**, 86-101.

Ohira H., (1994). Inference of parent rocks by means of zircon crystal morphology and major element composition of host rocks - An example of granitic mylonites within the Tanakura Shear Zone -. *J. Geol. Soc. Japan*, **100**, 495-504.

Reviewer

D. Miallier

Absorbed dose fraction for ^{87}Rb β particles

M.L. Readhead
Defence Science and Technology Organisation, P.O. Box 44, Pyrmont, NSW, 2009, Australia

(Received 4 April 2002; in final form 14 July 2002)

Abstract: *The dose absorbed by spherical quartz grains containing rubidium is calculated for grain diameters from 5 μm to 100 mm. The equivalent geometric factor as a function of grain diameter is also given.*

Introduction

Recently it was stated (Huntley and Hancock, 2001) that a clear need exists for a proper calculation of the absorbed energy fraction for β particles emitted by ^{87}Rb from within grains of various sizes. The tools required for such a calculation have previously been published (Readhead, 1987; with an *erratum* noted in *Ancient TL* **6**, p.20), but as this work was not referenced in the review by Adamiec and Aitken (1998), readers may not be familiar with it. A synopsis of the method is provided below, along with the results.

Theory

Spencer (1959) calculated the average energy dissipated near point isotropic sources of mono-energetic electrons and presented his numerical results in the form of a "de-dimensionalized energy distribution" $J(x)$, where x is the distance from the source in units of pathlength r_0. He calculated electron penetration taking into account both nuclear elastic scattering and electron slowing down, but did not include straggling. Charlton (1970) states that Spencer's results have been extensively tested by Cross (1967), and that "over a wide range of beta spectra there is excellent agreement between theory and experiment, except at distances from the source greater that about half of the range of the most energetic electrons in the spectrum. Within this distance about 95% of the total source energy is deposited."

The calculations of Spencer are the basis of absorbed dose distribution functions derived by both Berger (1971, 1973) and Charlton (1970). The method of Berger has previously been used by Mejdahl (1979); that of Charlton by Bell (1978, 1979). Both are equivalent and Bell (1979) found good agreement between his and Mejdahl's results. The approach of Charlton is followed here.

Consider a sphere of diameter D containing a homogeneous distribution of point sources, surrounded by a region not containing any sources, as in Figure 1.

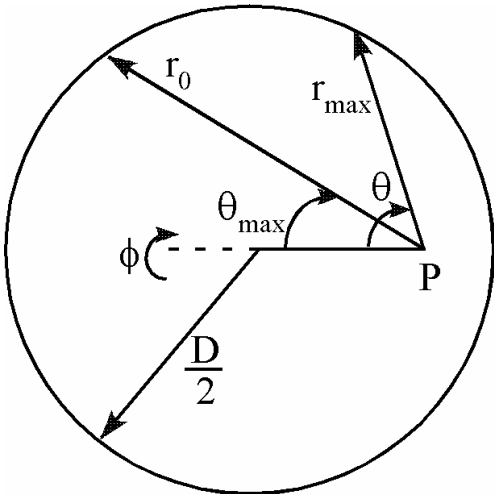

Figure 1.
Geometry for a spherical absorber which emits N_0 electrons per unit mass. It is surrounded by a region which does not emit electrons.

Within the sphere N_0 electrons are emitted per unit mass, each of initial energy E_0 and pathlength r_0. Using Spencer's results, Charlton showed that the energy dissipated per unit volume at point P is

$$D_e(r) = N_0 E_0 S_e(r) \tag{1}$$

where (after some manipulation) the spherical geometrical function

$$S_e(r) = 1 - \frac{1}{2}\int_{\theta_{\max}}^{\pi} \left(1 - \frac{\int_0^{r_{\max}} J(x)\,dx}{\int_0^1 J(x)\,dx}\right) \sin\theta \; d\theta \tag{2}$$

is obtained. Here D is the diameter of the grain, r is the distance from the centre of the grain to P,

$$r_{\max} = r\cos\theta + \sqrt{\left(D/2\right)^2 - \left(r\sin\theta\right)^2} \tag{3}$$

is the distance from P to the edge of the grain for an angle θ and

$$\theta_{\max} = \begin{cases} 0 \text{ for } r_0 > D/2 + r \\ \arccos\left[\dfrac{r^2 + r_0^2 - \left(D/2\right)^2}{2rr_0}\right] \text{ otherwise.} \end{cases} \quad (4)$$

Equation (1) gives the dose absorbed at a point. The mean dose absorbed by a spherical grain is

$$\langle D_e \rangle = N_0 E_0 \langle S_e \rangle \quad (5)$$

where

$$\langle S_e \rangle = \frac{\int_0^{2\pi}\int_0^{\pi}\int_0^{D/2} S_e r^2 \sin\theta dr d\theta d\phi}{\int_0^{2\pi}\int_0^{\pi}\int_0^{D/2} r^2 \sin\theta dr d\theta d\phi} \quad (6)$$

When a nuclide decays and emits a β particle, that particle can have a range of possible energies up to a maximum value E_{max}. The mean dose absorbed from a β particle must be averaged over this spectrum, so

$$\langle D_\beta \rangle = N_0 \langle E_\beta \rangle \quad (7)$$

where

$$\langle E_\beta \rangle = \frac{\int_0^{E_{\max}} \langle S_e \rangle E n(E) dE}{\int_0^{E_{\max}} n(E) dE}. \quad (8)$$

$n(E)dE$ is the number of β particles emitted per unit energy with initial energies in the interval E to E+dE. For many transitions the energy distribution of the spectrum is not fully known, but Murthy (1971) gives formulae for calculating it.

Computational considerations

To evaluate the above equations the β particle maximum energies and intensities, and internal conversion and Auger electron energies and intensities can be obtained from the Nuclear Data Retrieval Program (http://www.nndc.bnl.gov/). The pathlengths in quartz can be derived from the tables of Pages *et al.* (1972).

Spencer's $J(x)$ was evaluated for electrons with initial energies of 0.025, 0.05, 0.1, 0.2, 0.4, 0.7, 1, 2, 4 and 10 MeV traversing selected media, including carbon (Z=6) and aluminium (Z=13) using a mesh in x of $\Delta x = 0.025$. To interpolate in x requires the use of a quadratic interpolation formulae. To interpolate for quartz at a particular initial energy one uses

$$\frac{\ln J_q(x)}{A_q} = \left[\frac{\ln J_a(x)}{A_a} - \frac{\ln J_c(x)}{A_c}\right]\left(\frac{Z_q - Z_c}{Z_a - Z_c}\right) + \frac{\ln J_c(x)}{A_c} \quad (9)$$

and

$$A_q = A_c + (A_a - A_c)\left(\frac{Z_q - Z_c}{Z_a - Z_c}\right) \quad (10)$$

where the subscripts q, c and a refer to Z, $J(x)$ and constants A (given by Spencer) for quartz, carbon and aluminium, respectively. To interpolate in initial energy one uses:

$$\frac{\ln J(x)}{A} = \left[\frac{\ln J_{UE}(x)}{A_{UE}} - \frac{\ln J_{LE}(x)}{A_{LE}}\right]\left(\frac{\log E - \log E_L}{\log E_U - \log E_L}\right) + \frac{\ln J_{LE}(x)}{A_{LE}} \quad (11)$$

and

$$A = A_{LE} + (A_{UE} - A_{LE})\left(\frac{\log E - \log E_L}{\log E_U - \log E_L}\right) \quad (12)$$

where E is the energy of interest, bracketed above by E_U and below by E_L, with associated $J_{UE}(x)$ and $J_{LE}(x)$, and A_{UE} and A_{LE}.

For Z=37 Murthy gives the β energy spectrum as:

$$n(E)dE = k\left(1.7964 + 8.4692E + 6.8327E^2\right)\left(E_{\max} - E\right)^2 dE \quad (13)$$

where k is a constant.

Results

For ^{87}Rb the maximum β energy is 0.2823 MeV. Table 1 shows the absorbed dose in MeV/N_0 and μGy/a/(ppm Rb) for grain diameters from 5μm to 100 mm. Since the values are obtained after averaging over the β spectrum, a simple geometric factor cannot be given. However, an equivalent value is obtained if $\langle S_e \rangle$ is set to 1 in Equation (8), in which case the absorbed dose is 0.0825 MeV/N_0 or 0.3580 μGy/a/(ppm Rb). This leads to the equivalent geometric factors shown in the table for each diameter. Of course, for very large grains this same maximum absorbed dose is achieved, as the geometric factor approaches 1. Figure 2 plots the equivalent geometric factor as a function of grain diameter.

Note that the results apply to an absorber of quartz, for which $Z_q \approx 10.8$. Slightly different results will be obtained with other absorbers, by using the appropriate effective atomic number in Equations 9 and 10.

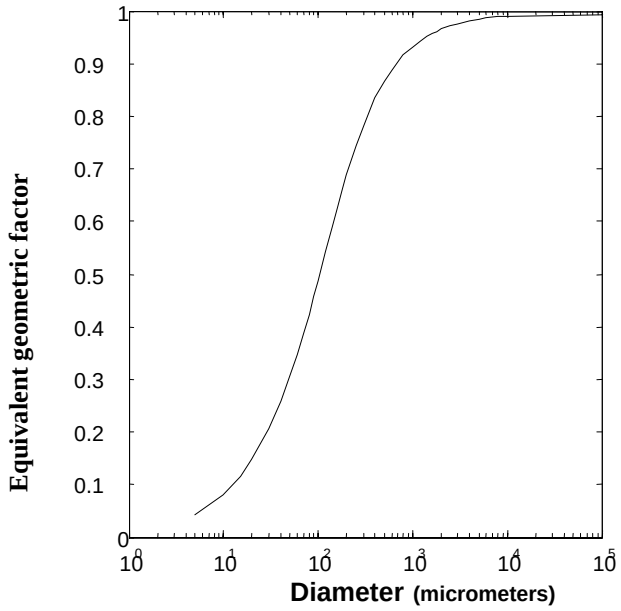

Figure 2.
Equivalent geometric factor as a function of grain diameter for a quartz grain containing an homogeneous distribution of ^{87}Rb

In addition it should be pointed out that the ^{87}Rb β energy spectra is most likely an approximation on the part of Murthy, due to the paucity of experimental data. His paper includes correction factors for various types of forbiddingness, but doesn't specifically mention ^{87}Rb. However, an approximate result based on his spectra is better than no result at all, and is certainly an improvement over that of Bell (1979), who only used the average β energy for ^{87}Rb when calculating the attenuation factor for 100 μm quartz grains.

Diameter (mm)	Absorbed dose (MeV/ N_0)	Absorbed dose μGy/a/(ppm Rb)	Equivalent geometric factor
0.005	0.0036	0.015	0.043
0.01	0.0067	0.029	0.081
0.015	0.0095	0.041	0.115
0.02	0.0121	0.053	0.147
0.03	0.0169	0.073	0.205
0.04	0.0212	0.092	0.257
0.05	0.0251	0.109	0.305
0.06	0.0287	0.125	0.348
0.07	0.0320	0.139	0.388
0.08	0.0350	0.152	0.424
0.09	0.0377	0.164	0.457
0.1	0.0402	0.175	0.488
0.12	0.0447	0.194	0.542
0.14	0.0485	0.211	0.588
0.16	0.0517	0.225	0.627
0.18	0.0545	0.236	0.660
0.2	0.0568	0.247	0.689
0.25	0.0614	0.267	0.744
0.3	0.0646	0.281	0.784
0.4	0.0689	0.299	0.835
0.5	0.0715	0.311	0.867
0.6	0.0733	0.318	0.889
0.8	0.0755	0.328	0.916
1	0.0769	0.334	0.932
1.2	0.0778	0.338	0.943
1.4	0.0785	0.341	0.951
1.6	0.0789	0.343	0.957
1.8	0.0793	0.344	0.962
2	0.0796	0.346	0.965
2.5	0.0802	0.348	0.972
3	0.0805	0.350	0.976
4	0.0809	0.352	0.981
5	0.0812	0.353	0.984
6	0.0814	0.353	0.987
8	0.0816	0.354	0.989
10	0.0817	0.355	0.990
100	0.0819	0.355	0.992

Table 1. *Absorbed dose and equivalent geometric factor as a function of grain diameter for a quartz grain containing an homogeneous distribution of ^{87}Rb.*

References

Adamiec, G. and Aitken, M. (1998). Dose-rate conversion factors: update. *Ancient TL* **16**, 37-50.

Bell, W.T. (1978). *Studies in thermoluminescence dating in Australasia*, unpublished PhD thesis, Australian National University.

Bell, W.T. (1979). Attenuation factors for the absorbed radiation dose in quartz inclusions for thermoluminescence dating. *Ancient TL* **8**, 2-13.

Berger, M.J. (1971). Distribution of absorbed dose around point sources of electrons and beta particles in water and other media. *J. Nuclear Medicine*, Supplement No. 5, MIRD Pamphlet no. 7, 7-23.

Berger, M.J. (1973). Improved point kernels for electron and beta-ray dosimetry. *NBSIR*, Natl Bur Stand., Washington D.C., 73-107.

Charlton, D.E. (1970). Energy dissipation near an interface: a more realistic approach to electron range and stopping power. *Radiat. Res*. **44**, 575-593.

Cross, W.G. (1967). The distribution of absorbed energy from a point beta source, *Can. J. Phys.* **45**, 2021-2040.

Huntley, D.J. and Hancock, R.G.V. (2001). The Rb contents of the K-feldspar grains being measured in optical dating. *Ancient TL* **19**, 43-46.

Mejdahl, V. (1979). Thermoluminescence dating: beta-dose attenuation in quart grains. *Archaeometry* **21**, 61-72.

Murthy, M.S.S. (1971). Shape and average energy of beta-particle spectra. *Int. J. Appl. Radiat. Isotopes* **22**, 111-123.

Pages, L., Bertel, E., Joffre, H. and Sklavenitis, L. (1972). Energy loss, range and bremsstrahlung yield for 10 keV to 100 MeV electrons in various elements and chemical compounds. *At. Data* **4**, 1-127.

Readhead, M.L. (1987). Thermoluminescence dose rate data and dating equations for the case of disequilibrium in the decay series. *Nucl. Tracks Radiat. Meas.* **13**, 197-207.

Spencer, L.V. (1959). Energy dissipation by fast electrons. *Natn. Bur. Stand. Monogr*. **1**.

Reviewer

Jean Faïn

Jubilee Aitken - an eightieth birthday celebration

10 - 12 April 2002

It is given to very few of us to be the founder of a new branch of science.

Martin Aitken is one of those.

From a background in synchrotron physics at the Clarendon Laboratory, Oxford he moved to the infant Research Laboratory for Archaeology and the History of Art, known to most of us "RLAHA" or as "Keble Road". There he devoted his attention to a variety of physical methods of aiding the archaeologist. It was he who, with Christopher Hawkes, coined the word *Archaeometry* for the application of mathematics and physics to archaeological problems. He first devoted his attention to archaeomagnetism and its applications in this context, particularly proton magnetometer detection of buried remains. Since then, of course, Archaeometry has come, by extension, to embrace the application of all the sciences, and the original archaeology has been joined by Quaternary geology in the field of operations. Aitken is a physicist and it may therefore not be coincidental that a goodly proportion of the advances in methodology for luminescence dating have been made by physicists.

At the time, thermoluminescence was fairly well-known as a tool for studying minerals *per se*. Taking up an abandoned speculation that it should be possible to use mineral thermoluminescence to find the age of pottery, he showed that it was indeed possible to do so, although by his own account he wondered from time to time whether it was going to be possible after all. Nowadays, pottery features rather infrequently in the dating game, if you exclude the art market and authentication or the lids of toilet cisterns from Pripyat, as reported to the Conference.

The needed skills gradually diffused out from Oxford in the notebooks and heads of their many visitors and, by the mid seventies, thermoluminescent dating laboratories were beginning to spring up elsewhere in the UK, in continental Europe and even as far away as Australia and Canada. Visitors to those laboratories could not help but be struck by the fact that the way things are/were done could be identifiably traced to the Keble Road influence. Indeed, it was only in the 1990s that it was possible to find a luminescence dating laboratory in which such influence was no longer direct.

Two big advances were responsible for the expansion into geology:
1) the realisation by the Simon Fraser group and independently in the USSR, that the luminescence clock could be reset by exposure of mineral grains to sunlight and that this would allow sediments to be dated by TL and,
2) the corollary that, just as TL can be used to date samples for which the TL clock has been reset by heat, so photostimulation can be used to date samples for which the clock has been reset by light exposure. Resetting by heat is, of course still permitted.

All of these have a direct line of descent from Martin Aitken.

Now he has reached his eightieth birthday, not perhaps a Jubilee in the dictionary sense, but who cares?

It was therefore appropriate for his former students and colleagues to gather together in Clermont-Ferrand, to help celebrate it. For the idea and the execution, great credit and our thanks are due to Stephen Stokes and Didier Miallier.

Some forty five of us were there. There were a number of his earliest students, including his first D Phil student, Mike Tite, and others from the early years. There were present-day students of his students; and others who had taken the Golden Road to Keble Road from other less favoured climes and places. Unless my arithmetic is wrong, there was someone present who had worked at Keble Road for every year that Martin was there. Absent friends sent greetings by video and word processor. The writer of these notes can claim to have known Martin longer than anyone else (1950) and have travelled furtherest to get there. Many recalled the hospitality of Martin and Joan at Islip and expressed regrets that she was unable to be present.

The celebration took the form of a two-day conference with papers grouped roughly in eight themes. The general idea was to present the current

state of the art with invited and contributed papers and, in due time, to present Martin with a book containing them. Perhaps it could be regarded as the book that he himself might write were he updating his celebrated 1985 and 1998 books. It is hoped that it will be as useful to practitioners as those two were. The programme is reproduced below.

A "family tree" with the names of all his students and their students, in the form of a framed picture was presented. And individuals added their personal gifts.

There was also a good deal of food and wine.

Happy Birthday, Martin!

John Prescott
Physics Department
University of Adelaide

email: jprescot@physics.adelaide.edu.au

Program

Thursday 11th April

Stephen Stokes & Didier Miallier Introduction & welcome
John Prescott A datable friendship?
Rainer Grün & Geoff Duller The place of luminescence dating in the context of absolute dating techniques
Steve McKeever & Richard Bailey The theoretical framework for luminescence dating
Ludwig Zöller Towards high temporal resolution of loess: Combination of physical numerical dating (luminescence and ^{14}C) and relative chronologies (magnetism and isotopes)
Richard Bailey, Barney Smith, Andrew Murray & Ann Wintle Luminescence properties of quartz relevant to dating applications
Ann Wintle, & Geoff Duller Luminescence properties of feldspar relevant for dating applications
Raphaël Visocekas Luminescence in France & its connection with Martin Aitken
Morteza Fattahi, Raphaël Visocekas & Didier Miallier Red luminescence - new approaches and potentials
Antoine Zink Far red luminescence of feldspar
John Prescott Something old & something new: Some new data on Thick Source Alpha Counting and some cosmic reflections
Ian Bailiff & Yeter Göksu Accident dosimetry
Lars Bøtter-Jensen, John Prescott & Nigel Spooner Instrumentation for the detection of luminescence emissions
Stephen Stokes A celebration of the career and contributions of Martin Aitken FRS

Friday April 12

Geoff Duller, Li ShengHua & Andrew Murray Single aliquot and single grain equivalent dose determination
Helen Bray, Geoff Duller, Richard Bailey & Stephen Stokes Data visualisation and error analysis in luminescence dating measurements
Joy Singarayer & Lars Bøtter-Jensen Linear modulation of optically-stimulated luminescence (LM-OSL)
Stephen Stokes and Simon Armitage Luminescence dating in desert sedimentary environments
Helen Roberts, Ann Wintle and Ludwig Zöller Luminescence dating of loess
Jakob Wallinga and Andreas Lang Beyond aeolian sediments: Applications of luminescence dating in fluvial and colluvial environments
Eddie Rhodes, Hélène Valladas and Norbert Mercier Luminescence dating frameworks for archaeological sciences in the Palaeolithic period
David Sanderson, Iona Anthony and Anne Sommerville The nature of the event: Luminescence dating in neolithic and later archaeology
Gunther Wagner Luminescence dating of sediment: An important tool in geoarchaeology
Andrew Murray, Roger Nathan and John Prescott Radioisotopes, dosimetry and dose rate determination
Dorothy Godfrey-Smith Plus ça change: A longitudinal study of developments in optical dating from the perspective of Rose Cottage Cave, South Africa
Hélène Valladas, Georges Valladas, Norbert Mercier, Chantal Tribolo TL dating of burnt stones
Marco Martini A database of TL dates on the Web

SFU age list

D. J. Huntley
Physics Dept., S.F.U., Burnaby, B.C., V5A 1S6, Canada.

A list of optical and thermoluminescence ages obtained at SFU up to the present can be found at http://www.sfu.ca/physics/research/workarea/huntley/ as a PDF file. If anyone would like a printed list, please ask me for one.

The following table is an outline of what is in the age list. O means optical dating, TL means conventional thermoluminescence dating, and TLS means thermoluminescence sediment dating. For most of the optical ages, 1.4 eV (IR) excitation of K-feldspars was used, and some ages have been corrected for anomalous fading; for a small number, 2.4 eV (green) excitation of quartz was used. Some samples for which no age was calculated are included in the age list, but not included in this table.

Region	type of sample	number of samples
Canada		
British Columbia	silt and sand, organic-rich sediment tsunami-laid sand or flood deposit glaciofluvial or glaciolacustrine silt pot sherd tephra	20 O, 3 TLS 10 O 13 O, 11 TLS 1 TL 4 TL
Alberta	aeolian sand delta sand, glaciolacustrine silt	10 O 2 O
Saskatchewan	aeolian sand	37 O
Manitoba	aeolian sand	11 O
Ontario	glacial sediments	3 TLS
Quebec	silt	1 O, 20 TLS
New Brunswick	dune sand	9 O, 1 TLS
Northwest Territory	dune sand, sand wedge	2 O
Yukon	tephra	1 TL
U.S.A.		
Alaska	tephra	1 TL, 1 TLS
Washington	peat, tsunami-laid deposit tephra	4 O 3 TL
Oregon	tsunami-laid lake deposits	5 O
California	sand and silt hearth	4 O 1 TL
Utah	tephra	1 TL
Massachusetts	beach dune	24 O
other		
South Australia	dune sands	16 O, 23 TLS
Siberia	sand, quartzite	3 O
Oceania	pot sherds	6 TL
ocean and gulf	sediment cores	19 TLS

10th International Conference on Luminescence and Electron Spin Resonance Dating Reno, Nevada, June 24-28, 2002

Student awards

The Vagn Mejdahl **poster award was shared by**

Gunter Erfut
Saxon Academy of Sciences
Freiberg, Germany

and

Sebastien Huot
Departement des Sciences de la Terre et de l'Atmosphère
Montréal, Canada

The **Martin Aitken** oral presentation award was shared by

Joy Singarayer
School of Geography and the Environment
Oxford, U.K.

and

Kristina Thomsen
Risø National Laboratory
Roskilde, Denmark

The prizes were presented by Dr Glenn Berger and the awards were sponsored by Risø National Laboratory, Denmark and by Daybreak Nuclear and Medical Systems Inc., U.S.A.

Bibliography

(from 1st October 2001 to 30th March 2002) Compiled by Ann Wintle

---

Alexanderson H., Hjort C., Moller P., Antonov O., and Pavlov M. (2001) The North Taymyr ice-marginal zone, Arctic Siberia - preliminary overview and dating. *Global and Planetary Change* **31**, 427-445.

Arbogast A. F., Wintle A. G., and Packman S. C. (2002) Widespread middle Holocene dune formation in the eastern Upper Peninsula of Michigan and the relationship to climate and outlet-controlled lake level. *Geology* **30**, 55-58.

Bartoll J., Rink W. J., and Schwarcz H. P. (2001) ESR signals from clusters of iron ions as indicators of the thermal history of fault gouge. *Applied Magnetic Resonance* **20**, 519-530.

Berger G. W., Pillans B. J., and Tonkin P. J. (2001) Luminescence chronology of loess-paleosol sequences from Canterbury, South Island, New Zealand. *New Zealand Journal of Geology and Geophysics* **44**, 501-516.

Bulur E., Duller G. A. T., Solongo S., Bøtter-Jensen L., and Murray A. S. (2002) LM-OSL from single grains of quartz. *Radiation Measurements* **35**, 79-85.

Burbidge C. I., Batt C. M., Barnett S. M., and Dockrill S. J. (2001) The potential for dating the Old Scatness site, Shetland, by optically stimulated luminescence. *Archaeometry* **43**, 589-596.

Chen X. Y., Spooner N. A., Olley J. M., and Questiaux D. G. (2002) Addition of aeolian dusts to soils in southeastern Australia: red silty clay trapped in dunes bordering Murrumbidgee River in the Wagga Wagga region. *Catena* **47**, 1-27.

Chithambo M. L. and Galloway R. B. (2001) On the slow component of luminescence stimulated from quartz by pulsed blue light-emitting diodes. *Nuclear Instruments and Methods in Physics B* **183**(358-368).

Chithambo M. L. and Galloway R. B. (2001) Some properties of luminescence lifetimes from quartz stimulated by blue light. *Radiation Effects and Defects in Solids* **154**, 361-365.

Chithambo M. L. and Galloway R. B. (2001) Temperature dependence of luminescence lifetimes in quartz under pulsed blue light stimulation. *Radiation Effects and Defects in Solids* **154**, 355-359.

Chivas A. R., Garcia A., van der Kaars S., Couapel M. J. J., Holt S., Reeves J. M., Wheeler D. J., Switzer A. D., Murray-Wallace C. V., Banerjee D., Price D. M., Wang S. X., Pearson G., Edgar N. T., Beaufort L., de Deckker P., Lawson E., and Cecil C. B. (2001) Sea-level and environmental changes since the last interglacial in the Gulf of Carpentaria, Australia: an overview. *Quaternary International* **83-5**, 19-46.

Chruscinska A., Oczkowski H. L., and Przegietka K. R. (2001) The optical bleaching of thermoluminescence in K-feldspar. *Journal of Physics D: Applied Physics* **34**, 2939-2944.

Clarke M., Rendell H., Tastet J.-P., Clavé B., and Massé L. (2002) Late-Holocene sand invasion and North Atlantic storminess along the Aquitaine Coast, southwest France. *The Holocene* **12**, 231-138.

Clemmensen L. B., Murray A. S., Beck J. H., and Clausen A. (2001) Large-scale aeolian sand movement on the west coast of Jutland, Denmark in late Subboreal to early Subatlantic time -a record of climate change or cultural impact? *GFF* **123**, 193-203.

Corazza M., Pratesi G., Cipriani C., Lo giudice A., Rossi P., Manfredotti C., Pecchioni E., Manganelli del fa C., and Fratini F. (2001) Ionoluminescence and cathodoluminescence in marbles of historic and architectural interest. *Archaeometry* **43**, 439-446.

de Lima J. F., Navarro M. S., and Valerio M. E. G. (2002) Effects of thermal treatment on the TL emission of natural quartz. *Radiation Measurements* **35**, 155-159.

English P., Spooner N. A., Chappell J., Questiaux D. G., and Hill N. G. (2001) Lake Lewis basin, central Australia: environmental evolution and OSL chronology. *Quaternary International* **83-5**, 81-101.

Fattahi M. and Stokes S. (2001) Luminescence dating of Quaternary volcanic events. *Oxford University School of Geography Research Papers* **58**, 1-72.

Frechen M., Neber A., Dermann B., Tsatskin A., Beonigk W., and Ronen A. (2002) Chronostratigraphy of aeolianites from the Sharon Coastal Plain of Israel. *Quaternary International* **89**, 31-44.

Frechen M., Vanneste K., Verbeeck K., Paulissen E., and Camelbeeck T. (2001) The deposition history of the coversands along the Bree Fault Escarpment, NE Belgium. *Geologie en Mijnbouw* **80**, 171-185.

Fukuchi T. and Imai N. (2001) ESR and ICP analyses of the DPRI 500 m drill core samples penetrating through the Nojima Fault, Japan. *Island Arc* **10**, 465-478.

Galloway R. B. (2002) Luminescence lifetimes in quartz: dependence on annealing temperature prior to beta irradiation. *Radiation Measurements* **35**, 67-77.

Glennie K. W. and Singhvi A. K. (2002) Event stratigraphy, paleoenvironment and chronology of SE Arabian deserts. *Quaternary Science Reviews* **21**, 853-869.

Göksu H. Y., Degteva M. O., Bougrov N. G., Meckbach R., Haskell E. H., Bailiff I. K., Bøtter-Jensen L., Jungner H., and Jacob P. (2002) First international intercomparison of luminescence techniques using samples from the Techa river valley. *Health Physics* **82**, 94-101.

Gore D. B., Rhodes E. J., Augustinus P. C., Leishman M. R., Colhoun E. A., and Rees-Jones J. (2001) Bunger Hills, East Antarctica: ice free at the Last Glacial Maximum. *Geology* **29**, 1103-1106.

Gozzi G., Costa A. A., Tatumi S. H., Kassab L. R. P., Momose E. F., Munita C. S., and Paiva R. P. (2001) Study of the thermoluminescence and optical stimulated luminescence properties of quartz crystal. *Radiation Effects and Defects in Solids* **154**, 347-353.

Grün R. (2002) ESR dose estimation on fossil tooth enamel by fitting the natural spectrum into the irradiated spectra. *Radiation Measurements* **35**, 87-93.

Hall A. M., Gordon J. E., Whittington G., Duller G. A. T., and Heijnis H. (2002) Sedimentology, palaeoecology and geochronology of Marine Isotope Stage 5 deposits on the Shetland Islands, Scotland. *Journal of Quaternary Science* **17**, 51-67.

Heimsath A. M., Chappell J., Spooner N. A., and Questiaux D. G. (2002) Creeping soil. *Geology* **30**, 111-114.

Henriksen M., Mangerud J., Maslenikova O., Matiouchkov A., and Tveranger J. (2001) Weichselian stratography and glaciotectonic deformation along the lower Pechora River, Arctic Russia. *Global and Planetary Change* **31**, 297-319.

Henshilwood C. S., d'Errico F., Yates R., Jacobs Z., Tribolo C., Duller G. A. T., Mercier N., Sealy J. C., Valladas H., Watts I., and Wintle A. G. (2002) Emergence of modern human behavior: Middle Stone Age engravings from South Africa. *Science* **295**, 1278-1280.

Hetzel R., Niedermann S., Tan M., Stokes S., Kubik P. W., and Ivy-Ochs S. (2001) Slip rates of active thrusts in the Qilian Shan (China) based on 21Ne and 10Be exposure ages of Late Pleistocene alluvial fans and luminescence dating of Holocene loess deposits. *Journal of Asian Earth Sciences* **19**, 28-.

Hodgson D. A., Noon P. E., Vyverman W., Bryant C. L., Gore D. B., Appleby P., Gilmour M., Verleyen E., Sabbe K., Jones V. J., Ellis-Evans J. C., and Wood P. B. (2001) Were the Larsemann Hills ice-free through the Last Glacial Maximum? *Antarctic Science* **13**, 440-454.

Houmark-Nielson M., Demidov I., Funder S., Grosfjeld K., Kjaer K. H., Larsen E., Lavrova N., Lysa A., and Nielsen J. K. (2001) Early and Middle Valdaian glaciations, ice-dammed lakes and periglacial interstadials in northwest Russia: new evidence from the Pyoza River area. *Global and Planetary Change* **31**, 215-237.

Julig P. J., Long D. G. F., Schroeder H. B., Rink W. J., Richter D., and Schwarcz H. P. (1999) Geoarchaeology and new research at Jerf al_Ajla Cave, Syria. *Geoarchaeology* **14**, 821-848.

Kale Y. D., Gandhi Y. H., and Joshi T. R. (2002) Study of influence of pre-heat treatment on the thermoluminescence glow curve pattern and related trapping parameters of technologically important synthetic quartz specimen. *Indian Journal of Pure and Applied Physics* **40**, 107-110.

Lawson M. P. and Thomas D. S. G. (2002) Late Quaternary lunette dune sedimentation in the southwestern Kalahari desert, South Africa: luminescence based chronologies of aeolian activity. *Quaternary Science Reviews* **21**, 825-836.

Lebel S., Trinkaus E., Faure M., Fernandez P., Guerin C., Richter D., Mercier N., Valladas H., and Wagner G. A. (2001) Comparative morphology and paleobiology of Middle Pleistocene human remains from the Bau de l'Aubesier, Vaucluse, France. *Proceedings of the National Academy of Sciences* **98**(20), 11097-11102.

Li S. H. and Miao J. M. (2001) Effects of light exposure on the TL dating of pottery. *Science in China Series D - Earth Sciences* **44**, 1038-1042.

Lunkka J. P., Saarnisto M., Gey V., Demidov I., and Kiselova V. (2001) Extent and age of the Last Glacial Maximum in the southeastern sector of the Scandinavian Ice Sheet. *Global and Planetary Change* **31**, 407-425.

Mangerud J., Astakhov V. I., Murray A., and Svendsen J. I. (2001) The chronology of a large ice-dammed lake and the Barents-Kara Ice Sheet advances, Northern Russia. *Global and Planetary Change* **31**, 321-336.

Matsumoto H., Yamanaka C., and Ikeya M. (2001) ESR analysis of the Nojima fault gouge, Japan, from the DPRI 500 m borehole. *Island Arc* **10**, 479-485.

McKeever S. W. S. (2001) Optically stimulated dosimetry. *Nuclear Instruments and Methods in Physics B* **184**, 29-54.

Nott J. F., Thomas M. F., and Price D. M. (2001) Alluvial fans, landslides and Late Quaternary climatic change in the wet tropics of northeast Queensland. *Australian Journal of Earth Sciences* **48**, 875-882.

Oczkowski H. L. (2001) Gamma spectrometry for dose rate determination in luminescence dating. *Physica Scripta* **64**, 518-528.

Ogden R., Spooner N., Reid M., and Head J. (2001) Sediment dates with implications for the age of the conversion from palaeochannel to modern fluvial activity on the Murray River and tributaries. *Quaternary International* **83-5**, 195-209.

Ohta M. and Takami M. (2000) Thermoluminescent properties of tridymite SiO_2: Al^{3+}, Eu^{3+}. *Journal of Sol-Gel Science and Technology* **19**, 737-740.

Ollerhead J., Huntley D. J., Nelson A. R., and Kelsey H. M. (2001) Optical dating of tsunami-laid sand from an Oregon coastal lake. *Quaternary Science Reviews* **20**, 1915-1926.

Olsen L., Van der Borg K., Bergstrom B., Sveian H., Lauritzen S. E., and Hansen G. (2001) AMS radiocarbon dating of glacigenic sediments with low organic carbon content - an important tool for reconstructing the history of glacial variations in Norway. *Norsk Geologisk Tidsskrift* **81**, 59-92.

Owen L. A., Finkel R. C., and Caffee M. W. (2002) A note on the extent of glaciation throughout the Himalaya during the global Last Glacial Maximum. *Quaternary Science Reviews* **21**, 147-157.

Page K. J., Dare-Edwards A. J., Owens J. W., Frazier P. S., Kellett J., and Price D. M. (2001) TL chronology and stratigraphy of riverine source bordering sand dunes near Wagga Wagga, New South Wales, Australia. *Quaternary International* **83-85**, 187-193.

Pavlov P., Svendsen J. I., and Indrelid S. (2001) Human presence in the European Arctic nearly 40,000 years ago. *Nature* **413**, 64-67.

Polikreti K. and Maniatis Y. (2002) A new methodology for marble provenance based on EPR spectroscopy. *Archaeometry* **44**, 1-21.

Richter D., Mauz B., Bohner U., Weissmuller W., Wagner G. A., Freund G., Rink W. J., and Richter J. (2000) Luminescence dating of the Middle/Upper Palaeolithic sites 'Sesselfelsgrotte' and 'Abri I am Schulerloch', Altmuhltal, Bavaria. In *Neanderthals and Modern Humans* (ed. J. Orschiedt and C. Weniger), pp. 30-41.

Schurr M. R., Hayes R., and Bush L. L. (2001) The thermal history of maize kernels determined by electron spin resonance. *Archaeometry* **43**, 407-419.

Schwarcz H. P. and Rink W. J. (2001) Dating methods for sediments of caves and rockshelters. *Geoarchaeology* **16**, 355-371.

Shulmeister J., Shane P., Lian O. B., Okuda M., Carter J. A., Harper M., Dickinson W., Augustinus P., and Heijnis H. (2001) A long late-Quaternary record from Lake Poukawa, Hawke's Bay, New Zealand. *Palaeogeography, Palaeoclimatology, Palaeoecology* **176**, 81-107.

Singh A. K., Parkash B., Mohindra R., Thomas J. V., and Singhvi A. K. (2001) Quaternary alluvial fan sedimentation in the Dehradun Valley Piggyback Basin, NW Himalaya: tectonic and palaeoclimatic implications. *Basin Research* **13**, 449-471.

Spooner N. A. and Franklin A. D. (2002) Effect of the heating rate on the red TL of quartz. *Radiation Measurements* **35**, 59-66.

Sunta C. M., Ayta W. E. F., Chubaci J. F. D., and Watanabe S. (2001) A critical look at the kinetic models of thermoluminescence: I first order kinetics. *Journal of Physics D* **34**, 2690-2698.

Sunta C. M., Ayta W. E. F., Chubaci J. F. D., and Watanabe S. (2002) General order and mixed order fits of thermoluminescence glow curves - a comparison. *Radiation Measurements* **35**, 47-57.

Thomas D. S., Holmes P. J., Bateman M. D., and Marker M. E. (2002) Geomorphic evidence for late Quaternary environmental change from the eastern Great Karoo margin. *Quaternary International* **89**, 151-164.

Volkel J. and Mahr A. (2001) IRSL-dating of periglacial slope deposits: results from the Bayerische Wald (Bavarian Forest). *Zeitschrift fur Geomorphologie* **45**, 295-305.

Wallinga J., Murray A. S., Duller G. A. T., and Tornqvist T. E. (2001) Testing optically stimulated luminescence dating of sand-sized quartz and feldspar from fluvial deposits. *Earth and Planetary Science Letters* **193**, 617-630.

Whitley V. H. and McKeever S. W. S. (2001) Linearly modulated photoconductivity and linearly modulated optically stimulated luminescence measurements on Al_2O_3:C. *Journal of Applied Physics* **90**, 6073-6083.

Williams M., Prescott J. R., Chappell J., Adamson D., Cock B., Walker K., and Gell P. (2001) The enigma of a late Pleistocene wetland in the Flinders Ranges, South Australia. *Quaternary International* **83-5**, 129-144.

Ye Y., Diao S., Wu X., Chen X., and Gao J. (2001) Thermodynamical behaviour of E' centers in quartz from sediments: potential for palaeothermometry and geochronometry. *Applied Magnetic Resonance* **20**, 301-306.

Zhang D. D. and Li S. H. (2002) Optical dating of Tibetan hand- and footprints: an implication for the palaeoenvironment of the last glaciation of the Tibetan Plateau. *Geophysical Research Letters* **29**, 10.1029/2001GL013479.

Zhou W. J., Dodson J., Head M. J., Hou Y. J., Lu X. F., Donahue D. J., and Jull A. J. T. (2002) Environmental variability within the Chinese desert-loess transition zone over the last 20,000 years. *The Holocene* **12**, 107-112.